Xanthomonas campestris pv. *musacearum* bacterial infection induces organ-specific callose and hydrogen peroxide production in banana

Abubakar Sadik Mustafa,[1] Benison Tugume,[1] Jamilu E. Ssenku,[1] Paul Ssemanda,[1] Shahasi Y. Athman,[1] Hannington Oryem-Origa,[1,2] Jerome Kubiriba,[3] Savithramma P. Dinesh-Kumar,[4] and Arthur K. Tugume[1*]

[1]Department of Plant Sciences, Microbiology and Biotechnology, College of Natural Sciences, Makerere University, Kampala, P. O. Box 7062, Uganda.
[2]Department of Biological Sciences, Faculty of Science, Islamic University in Uganda, Mbale, P. O. Box 2555, Uganda.
[3]National Banana Research Program, National Agricultural Research Organization (NARO), Kampala, P.O. Box 7065, Uganda.
[4]Department of Plant Biology and The Genome Center, College of Biological Sciences, University of California, Davis, California, 1002 Green Hall, One Shields Avenue, USA.

***Corresponding author:** Arthur Tugume; E-mail: arthur.tugume@mak.ac.ug

Abstract

Xanthomonas campestris pv. *musacearum* (*Xcm*) bacteria cause banana *Xanthomonas* wilt (BXW), the most destructive disease of bananas in East and Central Africa. During early stages of infection in susceptible banana cultivars, incomplete systemic movement of *Xcm* limits bacterial colonization in the upper organs. Mechanistic basis of this delayed movement is unknown. We hypothesized that *Xcm* infection triggers basal pattern triggered immune (PTI) responses whose spatial and temporal variability along banana's anatomical structure

accounts for initially limiting *Xcm* in upper organs. Hence, we examined PTI responses such as callose deposition and hydrogen peroxide (H_2O_2) production in different organs in response to *Xcm* infection in BXW susceptible Kayinja and Mbwazirume banana cultivars and wild resistant progenitor *Musa balbisiana*. *Xcm*-induced callose increased and peaked at 14 days post inoculation (dpi) and 28dpi as assessed by fluorescence microscopy and enzyme-linked immunosorbent assays, respectively. The levels of *Xcm*-induced H_2O_2 and callose were highest in the pseudostems and corms, respectively, and were independent of host susceptibility or resistance to BXW. H_2O_2 production showed a biphasic transient pattern with an initial increase at 1-hour post *Xcm*-inoculation (hpi), followed by a decline 3-6hpi and then a second increase by 12hpi. Our findings point to organ-specific responses to *Xcm* infection in bananas. The corm which doubles as a subterranean parenating organ and interface between mother plants and lateral shoots, was the most responsive organ in callose production while the pseudostem was the most responsive organ in H_2O_2 production, suggesting the significance of these organs in banana response to BXW.

Keywords: Banana, Callose, *Xanthomonas campestris* pv. *musacearum,* Corm, Hydrogen peroxide, *Musa balbisiana*, *Xcm*-mediated defense, Fluorescence microscopy, and PAMP-triggered immunity.

Plant-pathogen interactions constitute an evolutionarily old “arms race” dynamic struggle between pathogens and plants in which the goal of the host plant is to remain healthy and productive (Jones & Dangl, 2006; Anderson et al., 2010; Wang et al., 2021). In this struggle, plants defend themselves by recognizing pathogen-associated molecular patterns (PAMPs) such as bacterial flagellin via host-pattern recognition receptors (PRRs) that trigger a basal defense response called PAMP-triggered immunity (PTI) (Jones & Dangl, 2006; Nicaise et

al., 2009; Dodds & Rathjen, 2010). PTI results into a myriad of defense responses such as oxidative burst, callose deposition, mitogen-activated protein kinase (MAPK) phosphorylation cascades and transcriptome re-programing (Altenbach & Robatzek, 2007; Schwessinger & Zipfel, 2008; Moore et al., 2011). To overcome PTI response, pathogens secrete effectors that interfere with PTI (Jones & Dangl, 2006; Dodds & Rathjen, 2010). Plants also have hundreds of *R* genes that mainly encode nucleotide-binding and leucine-rich repeat (NLR) proteins which recognize and interact with the pathogens' effectors and activate a more robust defense response called effector-triggered immunity (ETI) (Jones & Dangl, 2006; Dodds & Rathjen, 2010). ETI response is often associated with localized cell death at the site of pathogen infection called the hypersensitive response (HR) that curtails pathogen progression (Jones & Dangl, 2006; Nicaise et al., 2009).

During PTI, the production of reactive oxygen species (ROS) such as hydrogen peroxide (H_2O_2) is one of the early, rapid, transient and measurable events (Torres et al., 2006; Bigeard et al., 2015). H_2O_2 performs multiple functions in plant defense against pathogens. For example, it is involved in direct anti-microbial activities at the sites of pathogen invasion, cell-wall reinforcement via lignification and oxidative cross-linking of cell-wall polymers, synthesis of phytoalexins, triggering programmed cell death (PCD) during HR which restricts the spread of infection, signaling the induction and transduction of systemic acquired resistance in distal tissues, activation of defense genes, and is an essential component of the signal transduction cascade leading to numerous defense responses (Kuźniak & Urbanek, 2000; Torres et al., 2006; O'Brien et al., 2012; Wang et al., 2019). The consequence of PTI is to prevent microbial colonization by enhancing accumulation of callose (a 1,3-β-D-glucan polymer) between the cell wall and the plasma membrane and the plasmodesmata (Beckman et al., 1982; Cohen et al., 1990; Luna et al., 2011; Underwood, 2012; Malinovsky et al.,

2014). Callose is naturally involved in numerous routine plant biological processes (Piršelová & Matušíková, 2013; Nedukha, 2015). However, increased callose deposition in cell walls in response to pathogen infection prevents further microbial colonization (Beckman et al., 1982; Cohen et al., 1990; Underwood, 2012; Malinovsky et al., 2014; Voigt, 2014; Kashyap et al., 2020). By slowing pathogen invasion in the attacked tissue, callose deposition allows time for the induction of additional defense responses.

Studies of PTI in banana (*Musa* spp) in response to bacterial pathogen *Xanthomonas campestris* pv. *musacearum* (*Xcm*) infection are very limited. The xylem-limited *Xcm* (also recently re-designated as *Xanthomonas vascicola* pv. *musacearum, Xvm*) (Studholme et al., 2020) is the cause of banana *Xanthomonas* wilt (BXW) disease, the most destructive disease of banana in East and Central Africa (ECA), where the crop supports the livelihoods of more than 70 million people (Abele et al., 2007; Smith et al., 2008; FAOSTAT, 2017; Dotto et al., 2018; Nakato et al., 2018; Ocimati et al., 2019). Symptoms of BXW include progressive yellowing and wilting of leaves, premature and uneven ripening of fruits, and creamy-yellowish bacterial oozes that appear 5-20 min after cutting diseased pseudostems (Tushemereirwe et al., 2004; Smith et al., 2008). These symptoms develop rapidly and the infected plants wither and rot within 3-4 weeks under field conditions (Smith et al., 2008). Banana plants on the same mat (the mother plant, its lateral shoots, and underground corm) may all get infected because the *Xcm* bacteria have sufficient time to attack all the vital organs including the underground corm (Ssekiwoko et al., 2006a; Ocimati et al., 2015).

All cultivated banana varieties grown in ECA are susceptible to BXW (Ndungo et al., 2006; Ssekiwoko et al., 2006b; Tripathi et al., 2008). The progenitor of cultivated bananas, the inedible wild *Musa balbisiana* is the only source of resistance against BXW (Ssekiwoko et

al., 2006b; Ssekiwoko et al., 2015; Nakato et al., 2019). Currently, the molecular basis of resistance in *M. balbisiana* is not known. Considering the technical difficulties associated with introgression of BXW resistance from *M. balbisiana* into edible banana via conventional breeding, transgenic technologies are a more feasible tool to improve banana resistance against BXW (Tripathi et al., 2016; Tripathi et al., 2017). Alternatively, since *Xcm* bacteria show limited systemic movement even in susceptible genotypes (Ocimati et al., 2015), cultural methods such as single diseased stem removal (SDSR) (Kubiriba et al., 2014) may be effective in the management of BXW. In SDSR method, diseased plants are observed early for symptoms and aseptically removed from the mats by cutting them off at the soil level, which curtails the bacteria from crossing the corm tissue to attack the lateral shoots (Kubiriba et al., 2014; Blomme et al., 2017). Indeed, in early stages of flower-mediated *Xcm* infection, the bacteria are restricted to the upper parts of the true stem (Ssekiwoko et al., 2006a), indicating some unknown mechanism dampens bacterial invasion. Low bacterial loads in the corm together with latent *Xcm* infections were observed and assumed to be the cause of new BXW incidences in areas where the disease was previously controlled (Ocimati et al., 2013). Furthermore, Ocimati et al. (2015) showed incomplete systemic infection of *Xcm* in bananas, suggesting some PTI defenses against BXW. According to Tripathi et al. (2019), *Xcm* infection in banana may activate both PTI and ETI responses. Accordingly, our hypothesis is that *Xcm* infection triggers basal PTI responses whose spatial and temporal variability along banana's anatomical structure accounts for initially restricting *Xcm* in upper organs.

In this study, we investigated how bananas respond to *Xcm* infection under screenhouse conditions with respect to callose deposition and H_2O_2 production as early measurable events of PTI. The understanding of these defense responses is vital towards the production of BXW

resistant banana cultivars either through conventional breeding or genetic engineering technologies.

MATERIALS AND METHODS

Plant materials

This study was approved by Uganda National Council for Science and Technology with the reference number NS107ES. Three banana genotypes, Pisang Awak (known in Uganda as, and hereafter referred to as, Kayinja), Mbwazirume, and *Musa balbisiana* were used in this study. Kayinja is a beer banana (triploid genotype ABB), Mbwazirume is a cooking "matooke" type of the East African Highland banana (EAHB, triploid AAA-EA), while *M. balbisiana* is a wild and inedible banana (diploid genotype BB). Kayinja and Mbwazirume were selected for their known susceptibility to BXW, while *M. balbisiana* is resistant to BXW (Ssekiwoko et al., 2006b; Tripathi et al., 2008; Nakato et al., 2019). Kayinja and Mbwazirume represent genotypes that are predominantly grown in two contrasting banana cropping systems of ECA: the less-managed Kayinja-based system common in DRC, and highly managed East African Highland banana-based cropping system common in Uganda (Smith et al., 2008).

Healthy Kayinja, Mbwazirume and *M. balbisiana* mother plants that were used to generate explants for tissue culture of the experimental plants were obtained from farmer's fields in Mbarara, southwestern Uganda. These mother plants were identified phenotypically using standard procedures at the National Agricultural Research Laboratories (NARL) at Kawanda, Uganda. Voucher specimens for Kayinja, Mbwazirume and *M. balbisiana* were deposited in the Makerere University Herbarium with the deposition number ASM001, ASM002 and ASM003, respectively. Plantlets of these genotypes were raised from the explants through

standard tissue culture procedures at the Tissue Culture Laboratory of the NARL. The plantlets were weaned at 75% humidity in the humidity chamber for 1 month and hardened for 1 month before potting for establishment in a screen house. They were maintained in the screen house at the Banana Resource Centre at NARL under regular watering after every three days at atmospheric temperatures between 18°C to 30°C for 2.5 months prior to inoculation with *Xcm*.

Isolation and preparation of *Xcm* inoculum

The *Xcm* inoculum was isolated from a BXW infected Kayinja plant from a banana plantation at Kifu forest reserve, Mukono district, central Uganda. The presence of *Xcm* in the plant was confirmed using a lateral flow device (LFD) (DSMZ, Germany) according to manufacturer's instructions. The pseudostem was cut into short pieces of 0.5 m and left for 15-40 min to allow the yellowish sap to ooze-out of the cut surfaces. The bacterial ooze was carefully collected into 50 mL falcon tubes, immediately transferred into a cool box maintained at 4 ℃ and transported to the laboratory for analysis.

A part of the fresh yellowish ooze was serially diluted to 10-, 100-, 1000-, 10000- and 100000-fold with sterile distilled water and the rest of the fresh ooze was stored at 4 ℃. Aliquots of 100 µL of each of the dilutions were spread onto yeast extract peptone glucose agar (YPGA) containing 1% (w/v) yeast extract, 1% (w/v) peptone, 1% (w/v) glucose, 1.5% (w/v) agar, pH 7.0, and incubated for 48 hours at 28°C as described by Mwangi et al. (2007). Characteristic *Xcm* colonies that appeared yellow, mucoid and circular were sub-cultured further on a new YPGA medium to obtain pure *Xcm* colonies (Tripathi et al., 2007). To confirm whether the isolates were *Xcm*, DNA was extracted from the pure colonies using PureLink™ genomic DNA extraction kit (Thermo Fisher Scientific, USA) following

manufacturer's instructions and polymerase chain reaction (PCR) was run using *Xcm*-specific GspDm-F2/GspDm-R3 primers as described in Adriko et al. (2012). The PCR product was assessed by agarose gel electrophoresis and thereafter cleaned using the ExoSAP-IT™ PCR product cleanup kit (Applied Biosystems) following manufacturer's instructions. The cleaned PCR product was subjected to Sanger sequencing reactions using BigDye™ Terminator v3.1 cycle sequencing kit (Applied Biosystems) at the DNA sequencing facility of the Department of Plant Sciences, Microbiology and Biotechnology, Makerere University, Uganda. The DNA sequences generated were compared with the existing DNA sequences in the National Center for Biotechnology Information (NCBI) genebank using the Basic Local Alignment Search Tool (BLAST).

Inoculation of banana plants with *Xcm*

Banana plants at 2.5 months old were used for this study in a completely randomized design. The bacterial ooze stored at 4°C was retrieved after 5 days and diluted with sterile distilled water to OD_{600} = 2.5 (5 x 10^8 cells/mL). Experiments were performed in triplicate and repeated two times with similar results. Using 1 mL sterile syringes (BD Micro-Fine™ Plus, USA), 60 plants of each banana genotype were infiltrated with 200 µL of the *Xcm* inoculum (1 x 10^8 cells) on the dorsal side of leaf petioles as described by Ssekiwoko et al. (2006b). Additional 60 plants for each genotype were infiltrated with 200 µL of sterile distilled water and used as controls. Twenty-four plants of each genotype from the inoculated and control groups were used to examine callose deposition in the banana tissues using both fluorescence microscopy and Triple Antibody Sandwich Enzyme-linked immunosorbent assay (TAS-ELISA, hereafter referred to as ELISA). Additionally, 15 plants of each genotype from the inoculated and control groups were used for determination of H_2O_2 production by spectrophotometry and bright-field microscopy methods. The remaining 21 plants of each

genotype from the inoculated and control groups were left for further observations of BXW disease development. These plants were observed daily for 56 days and the time taken to show initial BXW symptoms and death of the entire plant were recorded. About 5 cm^2 of leaf tissue from the *Xcm*-inoculated and control groups were excised aseptically using sterile surgical blades and tested for *Xcm* at 0, 1, 2, 7, 14, 28 and 56 (dpi) by the LFD and PCR methods as described above.

Sampling

Destructive sampling was employed in the collection of samples from three *Xcm*-inoculated and three controls at 0, 1, 3, 6 and 12 hours post inoculation (hpi) for determination of H_2O_2 production by both spectrophotometry and bright-field microscopy methods. Similarly, tissue samples were collected at 0, 1, 2, 7, 14 and 28 days post inoculation (dpi) from a different set of plants for determination of callose production by both fluorescence microscopy and ELISA methods. For fluorescence microscopy, samples were quickly excised using sterile surgical blades from pseudostems (5cm long, longitudinally from the top, where the pseudostem starts), roots (5cm long, up to 5 different roots) and corms (2 cm wide, sliced longitudinally from the center). Samples for bright-field microscopy were collected from the inoculated leaves (6 cm long, from the leaf apex including the midrib), in addition to pseudostems and corms as described above. All the excised tissues were immediately immersed into formalin-acetic acid-alcohol (FAA) fixative solution, containing 50% (v/v) of ethanol, 5% (v/v) of acetic acid, 5% (v/v) of formalin and 40% (v/v) of sterile distilled water to preserve, de-stain and arrest any further metabolism in the tissues (Soukup & Tylová, 2014). The tissues were kept in the fixative at room temperature in the laboratory until they were de-stained (48-72 hours).

For the ELISA method and spectrophotometry methods, samples were quickly excised using sterile surgical blades from the inoculated leaves and the pseudostems (6 cm long, longitudinally from where sampling for fluorescence microscopy and bright-field microscopy stopped). Sampling of roots (not considered for spectrophotometry method) and corms were performed as stated above for fluorescence microscopy/bright-field microscopy. All the excised tissues were placed into well-labeled 50 mL falcon tubes and immediately immersed into liquid nitrogen. The samples were transported to the laboratory and stored at -80°C until subsequent processing. Owing to the transient nature of H_2O_2 in plant tissues (Noctor et al., 2015), all tissues were processed within 8-24 hours after collection.

Vacuum-infiltration and tissue sectioning

To further process the samples for fluorescence and bright-field microscopy, the tissues fixed in FAA were vacuum-infiltrated for 10 min to remove intercellular air from the tissues as described by Soukup and Tylová (2014). Vacuum infiltration was done using a vacuum pump (Model COM71/a, Coverco, Italy) connected to a glass desiccator. The vacuum-infiltrated tissues were recovered and up to 5 sections each of 100 µm thickness were made from each of the plant tissues using a sectioning knife (Dovo, Germany) and a hand-held microtome (MCT001, United Scientific Supplies, USA) as described by Soukup and Tylová (2014).

Staining and microscopy

The sections for determination of callose production were then stained in the dark for 2 hours in freshly prepared 0.01% aniline blue fluorochrome prepared in 150 mM K_2HPO_4 (Schenk & Schikora, 2015) while the sections for determination of H_2O_2 production were stained using the chromogen 3,3'-Diaminobenzidine (DAB) as described by Daudi and O'Brien (2012) with a few modifications. The modifications to the DAB-staining procedure included

subjecting the tissues to 8 min instead of 5 min of vacuum infiltration with DAB; 2 hours instead of 4 hours of shaking at 100 rpm and 300 µL instead of 200 µL of DAB reagent. These volumes were adjusted to enable better visibility of the DAB stain under the microscope. The sections were then rinsed using sterile water until the rinsing water was colorless. The clean tissue sections were then mounted on glass slides in a droplet of sterile water. The aniline blue-stained callose and DAB-stained H_2O_2 were visualized through fluorescence microscopy (using the DAPI filter at 365 nm excitation and 450nm emission) and bright-field microscopy, respectively. All microscopic observations were done under AxioScope A1 microscope (Carl-Zeiss, Oberkochen, Germany). Image acquisition, processing and management were conducted using ZEN 2.3 SP1 imaging software (Carl-Zeiss, Oberkochen, Germany). Up to four images were captured for each organ at 1,300 x 1,030 resolution in monochrome and in color formats. All images were captured at ×100 magnification and then converted to jpeg format for callose quantification and H_2O_2 localization.

Quantitative determination of callose by the Callosecounter software

To provide a quantitative estimate of callose observed under the microscope, the images obtained from fluorescence microscopy were all first converted to 8-bit and saved as TIFF before batch processing for callose quantification. Multiple rotational morphological processing (RMP) program, set up as a Callosecounter plugin for Icy software (Image Analysis Hub, Institut Pasteur, Paris, France) was used for callose quantification of the TIFF images as described by Kohari et al. (2016). The callose particles observed under fluorescence microscope were read and interpreted as callose particle counts per square millimeter (counts mm^{-2}) of the tissue sections.

Enzyme-linked immunosorbent assay and quantification of callose

The plant samples stored at -80 ℃ were retrieved in 2 months and extraction of callose from the tissues were performed according to Kohler et al. (2000) and Khaledi et al. (2018). The callose extracts were stored at -20 ℃ until further analysis. Triple Antibody Sandwich Enzyme-linked immunosorbent assay (TAS-ELISA) was used to quantify *Xcm*-induced callose deposition in the banana organs contained in the extracts (Engvall & Perlmann, 1971; Van Weemen & Schuurs, 1971; Anderson & McNellis, 1998; Hosseini et al., 2018). The ELISA plates (SARSTEDT AG & Co. KG, Germany) were prepared by coating wells with the primary coating antibody (1-3-β-glucan-directed mouse IgG, Biosupplies Australia Pty Ltd, Australia). To each well, 100 µL of the coating antibody were added and the plates were covered with aluminium foil and incubated overnight at 4°C. The plates were further processed by standard ELISA blotting and washing procedures (Hosseini et al., 2018) prior to the addition of test samples.

One-hundred microliters of the callose extracts were added to the designated wells of the plates in triplicates. Similarly, 100 µL of laminarin standard (Biosupplies Australia Pty Ltd, Australia) at concentrations of 90 mg/mL, 70 mg/mL, 50 mg/mL, 30 mg/mL, 10 mg/mL, 0.9 mg/mL, 0.7 mg/mL and 0.5 mg/mL were also added to the designated wells of the plates in quadruplets and used as a standard for callose quantification (Nelson & Lewis, 1974; Zvyagintseva et al., 1999; Rioux et al., 2007; Chen & Kim, 2009; Zhang et al., 2015). Blanks of 100 µL (prepared by mixing 1 M NaOH and blocking buffer at a ratio of 1:2) were also added to the designated wells in quadruplets. The plates were covered and incubated overnight at 4°C. The plates were allowed to warm to room temperature; blotting and washing of the plates were done as above. About 100 µL of diluted secondary antibody (1-3-

β-glucan-directed Mouse IgG, Biosupplies Australia Pty. Ltd., Australia) was added to the wells. The plates were covered with aluminium foil and incubated for 4 hours at 37°C after which the plates were allowed to cool to room temperature with blotting and washing procedure repeated as above. About 100 µL of the diluted detection (conjugated) antibody (anti-Mouse IgG-Alkaline phosphatase, Lasec International Ltd, South Africa) was added to the wells (Engvall & Perlmann, 1971; Hosseini et al., 2018). The plates were covered with aluminium foil and incubated overnight at 4°C. The plates were then allowed to warm to room temperature; blotting and washing of the plates were done as described above.

To quantify callose in the extracts by spectrophotometry, 100 µL of freshly prepared para-nitrophenyl phosphate (*p*NPP) (Lasec International Pty. Ltd., Cape Town, South Africa) at a concentration of 1 mg/mL was added to the wells and left to incubate at room temperature (Reen, 1994). After 30 min, the reactions were terminated by addition of 100 µL of freshly prepared 3 M NaOH (Reen, 1994). The plates were transferred to iMark Microplate Reader (BIO-RAD, Japan) and shaken at medium speed for 1 min and absorbances were read at 405 nm (Reen, 1994). The absorbance readings obtained from the laminarin standard (y-axis) and the known laminarin concentrations (x-axis) were used to plot a standard curve. A simple linear regression of laminarin absorbance at 405 nm against Log_{10} of laminarin concentration (µg/mL) was performed to obtain the standard curve, $Y = \beta_1 X + \beta_0$ (Y = callose absorbance at 405 nm, β_1 = slope of the regression line, X = Log_{10} [callose concentration in µg/mL] and β_0 = Y-intercept). Callose absorbance and concentrations were recorded as laminarin equivalents.

Extraction and quantification of H_2O_2

Hydrogen peroxide was extracted from tissues using a method described by Patterson et al. (1984). The amount of H_2O_2 in each of the extracts from the tissues was determined according to Zhou et al. (2006) with absorbance of extracts measured using a spectrophotometer (Model Nano Drop One^C U.V/Vis, Thermo Fisher scientific, USA) at 240 nm. To determine the actual concentration of H_2O_2 in the plant extracts, a standard H_2O_2 curve was produced. Aliquots of 2.5 mL of distilled water were dispensed into five 10 mL falcon tubes. A stock solution of H_2O_2 at 50% (w/v) was used to prepare serial dilutions. An aliquot of 2.5 mL of 50% H_2O_2 was dispensed into the first tube containing 2.5 mL of distilled water and mixed well to make a uniform solution of H_2O_2. The stock solution was then serially diluted each time by transferring 2.5 mL of the solution from the previous dilution into the subsequent five falcon tubes each containing the 2.5 mL of distilled water. The amount of H_2O_2 in each of the five serial dilutions was determined against distilled water as a blank and their respective absorbance recorded by a spectrophotometer at 240 nm. Absorbance values of the serially diluted H_2O_2 were plotted against their molar concentrations to generate a standard curve describing the Lambert-Beer relationship between absorbance and molar concentration (M) (Lambert, 1760; Beer, 1852) which was used to calculate the amount of H_2O_2 in the aliquots of the filtrate extracted from plant tissues.

Data analysis

All data analysis was conducted in R statistical package version 3.6.3 (R Core Team, 2020). The Shapiro-Wilk normality test and Levene's *F* test were used to check for normality of data distribution and homogeneity of variances ($\alpha = 0.05$), respectively. Where normality of distribution and/or homogeneity of variances were violated, the data were log transformed before Analysis of Variance (ANOVA) was performed and where log transformations did not solve these violations, Welch's ANOVA (assuming unequal variances) was instead used.

Data that were normally distributed and homoscedastic were analyzed using ANOVA at α = 0.05 followed by Tukey's *post hoc* test while data that violated homogeneity of variance were analyzed using Welch's ANOVA followed by Games-Howell *post hoc* test (Games & Howell, 1976) to show significant differences between the group means. Additionally, the fluorescence microscopy and ELISA data on callose were analyzed through factorial ANOVA to investigate the effect sizes of treatment, genotype, organ and time as well as their interaction on the total variance in callose production. Actual values were used for data presentation using excel tables and graphs (GraphPad Prism software version 8.0.2, GraphPad Software, San Diego, USA).

RESULTS

Susceptibility of host plants to *Xcm* and development of BXW

The identity of *Xcm* isolate collected from the field and used in this study was confirmed by PCR showing the expected amplicon size of approximately 265 base pairs (*data not shown*). Nucleotide sequence of the amplicon when compared with the DNA sequences in the NCBI database showed 100% identity to *Xanthomonas campestris* pv. *musacearum* NCPPB 4379 (accession number, CP034655.1).

Upon inoculation with the *Xcm* isolate, the plants developed wilting symptoms at varying rates with Kayinja plants showing earlier wilting symptoms, followed by Mbwazirume and *M. balbisiana* (Fig. 1). The three banana genotypes showed statistically significant differences in the mean number of dpi to first appearance of symptoms and death of entire plants (Welch's ANOVA, $F_{(4,18.28)}$=3045, $P < 0.001$, $n = 21$) (Fig. 1M). Symptoms were first characterized by necrosis around the site of inoculation, followed by drooping of the inoculated leaves, then widespread chlorosis and necrosis of the inoculated leaves that spread

to all leaves and the pseudostem and finally, death of the entire plant (Fig. 1). All inoculated plants of Kayinja and Mbwazirume experienced drooping of the *Xcm*-inoculated leaves as early as 11 dpi and 14 dpi, respectively (Fig. 1M). Further systemic spread of BXW disease symptoms and death of the entire plants for Kayinja and Mbwazirume were observed at 30 dpi and 39 dpi, respectively (Fig. 1M). On the contrary, only 4 out of 21 *M. balbisiana* plants experienced drooping of the inoculated leaves by 21 dpi, with no systemic disease progression observed; later, the 4 plants recovered and were asymptomatic as the control plants (Fig. 1). At 7 dpi, the leaves of the *Xcm*-inoculated Kayinja and Mbwazirume plants tested positive for *Xcm* using LFDs and PCR and at 14 dpi the leaves of *M. balbisiana* had tested positive for *Xcm*. However, at the termination of the experiment, 56 dpi, *M. balbisiana* tested negative for *Xcm* similar to control plants (Table 1).

Variations in callose production due to *Xcm*-inoculation

For callose quantification by fluorescence microscopy, the method developed by Kohari et al. (2016) was used while the standard curve of laminarin absorbance at 405 nm against known laminarin concentrations (Y = 0.5079*X - 0.04534, $r = 0.9988$, $r^2 = 0.9975$, $F_{(1,7)}=2845$, $P < 0.001$) was used to compute the unknown callose concentrations from the obtained callose absorbance at 405 nm (Supplementary Fig. S1A).

Treatment of the three banana genotypes with *Xcm* revealed significant variation in callose production between the *Xcm*-inoculated plants and the control plants by both fluorescence microscopy (ANOVA, $F_{(1,286)}=9.43$, $P = 0.0023$) and ELISA detection (Welch's ANOVA, $F_{(1,1062)}=25.75$, $P < 0.001$) (Table 2, Fig. 2, Supplementary Fig. S2). Although there was also a general increase in callose in the controls, the amounts were consistently lower than those in the inoculated plants (Table 2, Fig. 2, Supplementary Fig. S2A and 2B). Additionally,

inoculation of the plants with *Xcm* accounted for 3.2% of total variance in callose production as detected by fluorescence microscopy (Factorial ANOVA, $F_{(1,216)}$=1024.11, $P < 0.001$) or 0.7% of the total variance as detected by ELISA (Factorial ANOVA, $F_{(1,1046)}$=2228.38, $P < 0.001$) (Table 3).

Variations in callose production between the three banana genotypes

Interestingly, this study revealed significant variation in callose production between the three banana genotypes when analyzed by fluorescence microscopy method (ANOVA, $F_{(2,285)}$=3.049, $P = 0.049$) but not by the ELISA detection method (ANOVA, $F_{(2,1175)}$=1.30, P = 0.273) (Table 2, Supplementary Fig. S2). The trend of callose production in the three genotypes was consistent when fluorescence microscopy method was used for callose quantification showing consistently highest callose production in *M. balbisiana*, followed by Mbwazirume and lastly, Kayinja (Fig. 2). However, partial Eta squared (η^2) showed that genotype only accounted for 2.1% and 0.2% (effect size) of the total variance in the observed callose production by fluorescence microscopy and ELISA method, respectively (Factorial ANOVA, $P < 0.001$) (Table 3).

Variations in callose production between organs of different banana genotypes

Callose deposits were consistently observed as densely packed white fluorescing particles in the corm compared to few particles in the pseudostem (Fig. 3, Supplementary Fig. S3). Surprisingly, using ELISA method, callose was also detected in the roots even though no fluorescing callose particles had been observed in the roots by the fluorescence microscopy method (Table 2, Fig. 2 and 3, Supplementary Fig. S2 and S3). Therefore, for further analysis of fluorescence microscopy data, the root tissues were not considered. This study revealed significant differences in callose deposition in the banana organs by both fluorescence

microscopy method (Welch's ANOVA, $F_{(1,242.56)}$=853.07, $P < 0.001$) and ELISA detection method (Welch's ANOVA, $F_{(3,542.52)}$=1636.80, $P < 0.001$) with the corm producing 2- to 4-fold more callose deposition than roots, pseudostems and leaves (Table 2, Supplementary S2A and S2B). Quite interestingly, organs accounted for 74.9% of the total variance in callose production as observed by fluorescence microscopy (Factorial ANOVA, $F_{(1,216)}$=24027.78, $P < 2.2\times10^{-16}$; Table 3). The same observations were made using ELISA detection in which up to 79.3% of total variance in callose production was accounted for by the organs (Factorial ANOVA, $F_{(3,1046)}$=89779.53, $P < 2.2\times10^{-16}$, Table 3).

Effect of *Xcm* inoculation over time on callose production

This study showed that callose production was significantly different across the different time points when assessed by fluorescence microscopy (Welch's ANOVA, $F_{(5,131.23)}$=8.83, $P <$ 0.001). Significant differences in callose production across the sampling time points were also obtained when the ELISA method was used for callose quantification (Welch's ANOVA, $F_{(5,506.58)}$ = 55.62, $P < 0.001$) (Table 2). Interestingly, corms and pseudostems in all genotypes showed presence of constitutive callose at 0 dpi prior to *Xcm* inoculation (Table 2, Fig. 2, Supplementary Fig. S2A and S2B). Observations at 0 dpi by the fluorescence microscopy method indicated the presence of constitutive callose in the pseudostems and corms in the range of 12.20 to 13.22 and 35.91 to 38.31 particles mm^{-2}, respectively (Fig. 2A and 2C, Supplementary Fig. S2A). The ELISA method indicated constitutive callose production in the leaves, pseudostems, corms and roots in the range of 6.87-2132 µg/mL (Fig. 2B, 2D-2F, Supplementary Fig. S2B). Upon *Xcm* inoculation, callose production increased significantly ($P < 0.001$) and rapidly reaching a maximum of 17.36 to 34.85 and 47.64 to 73.31 particles mm^{-2} at 14 dpi in the pseudostems and corms, respectively, as analyzed by fluorescence microscopy (Fig. 2A and 2C).

On the contrary, the ELISA data showed slow increase in callose in the pseudostem as compared to the corms to a maximum of 555.86 to 6,540.30 and 1,778,609.36 to 8,673,866.36 µg/mL at 28 dpi for the pseudostem and corm, respectively (Fig. 2B and 2D). The leaves and roots analyzed by ELISA method showed a similar trend like the pseudostems and corms (Fig. 2E and 2F). In all cases, an initial increase in callose lasted for and peaked at 7 to 14 dpi and followed by a negligible increase observed at 28 dpi (Fig. 2A-2F).

Callose production attained statistically significant levels at 7 dpi as compared to 0 and 1 dpi but not 2 dpi and further increased though not significantly at 14 dpi and remained not significantly different until 28 dpi (Table 1, Supplementary Fig. S2A). Using ELISA, there was significant callose production at 2 dpi as compared to 0 dpi, which increased significantly at 7 dpi and 14 dpi and remained unchanged up to 28 dpi (Table 2, Supplementary Fig. S2B). ELISA showed a slow increase in callose 0 to 14 dpi, followed by a sharp increase up to 28 dpi, an exception being the slow decline in the pseudostems (7-28 dpi) and a sharp decline in the corms (14-28 dpi) of Kayinja (Fig. 2B and 2D). Interestingly, partial Eta squared (η^2) showed that time accounted for 13.3% and 13.8% of total variance in callose production as detected by fluorescence microscopy (Factorial ANOVA, $F_{(5,216)}$=853.44, $P < 0.001$) and ELISA (Factorial ANOVA, $F_{(5,216)}$=9363.88, $P < 0.001$), respectively (Table 3).

Interaction effects between treatment, genotype, organ and time on callose production

The interactions between all experimental variables showed statistically significant effects on callose production by fluorescence microscopy ($P = 1.5 \times 10^{-6}$) and the ELISA ($P = 2.2 \times 10^{-16}$) (Table 4). However, certain interactions contributed no variance (0.0%) in callose

production such as organ × treatment, organ × time × treatment (fluorescence microscopy), and genotype × treatment, time × treatment, genotype × organ × treatment (ELISA). Organ × time yielded the highest interaction effect by contributing 4.5% of the total variance in callose detection by ELISA. Additionally, organ and time which had the highest single-factor effects of 79.3% and 13.8%, respectively, had 4.5% effect due to their interaction (Factorial ANOVA, Table 4). In contrast, fluorescence microscopy data showed that time × treatment interaction contributed the highest interaction effect of 1.8% of the total variance in callose production (Factorial ANOVA, Table 4).

Histolocalization of H_2O_2 in *Xcm*-inoculated banana tissues

We investigated if Kayinja and Mbwazirume differ in terms of H_2O_2 production in response to *Xcm* infection by staining tissues with 3,3'-Diaminobenzidine (DAB). Tissue sections from *Xcm*-inoculated plants showed a relatively dense DAB stain compared to controls (Fig. 4), with an exception of pseudostem of Kayinja and corms of both Kayinja and Mbwazirume which showed DAB stain in controls (Fig. 4B, C and O). There was a tendency of the DAB stain accumulating in patches within areas surrounding vascular tissues of the pseudostems and leaves (Fig. 4D, E, G, H and P, Q, V, W). In contrast, the corms showed the presence of the stains in the form of vesicle-like structures that were randomly distributed across the corm tissue (Fig. 4C, F, I and O, R, U). There were only slight and subtle differences in intensity and frequency of the DAB stain between tissues over time post-infection with *Xcm*. For example, although tissues at 6 hpi show a consistent DAB stain across all tissues (Fig. 4G-I and S-U), this is not the case in the other time points.

Variations in H_2O_2 production in *Xcm*-inoculated banana tissues

Our study showed that H_2O_2 concentrations varied significantly between *Xcm*-inoculated and control plants (Welch's ANOVA, $F_{(1,125.13)}$=7.48, P = 0.007) (Table 4, Fig. 5, Supplementary Fig. S2C). Additionally, H_2O_2 concentration varied significantly between the different organs with the pseudostem producing the highest H_2O_2 as compared to the leaves and corm (Welch's ANOVA, $F_{(2,104.59)}$=3.88, P = 0.024) (Table 4, Fig. 5, Supplementary Fig. S2C). The ANOVA results also show that H_2O_2 production significantly varied across the sampling time points (Welch's ANOVA, $F_{(4,86.158)}$=25.94, P < 0.001) (Table 4, Fig. 5, Supplementary Fig. S2C). In studied tissues of both genotypes, there was an initial transient spike in H_2O_2 observed at 1 hpi, followed by a decline at 3 to 6 hpi, and then by another increase detected at 12 hpi (Fig. 5). There was a biphasic H_2O_2 production in the tissues of *Xcm*-inoculated plants which gave a peak of 10.21 to 18.92 mol/L at 1 hpi followed by a decrease to 2.44 to 4.81 mol/L at 6 hpi and a further increase of 5.71 to 15.42 at 12 hpi. Constitutive and differential production of H_2O_2 in the banana tissues at 0 hpi varied between 1.12 to 6.77 mol/L with the highest constitutive H_2O_2 production observed in the pseudostem tissues and lowest in the the corm tissues (Fig. 5). Control plants generally showed constant production of H_2O_2 in all the tissues between 3 to 12 hpi. These results also show that there was no significant difference in H_2O_2 production between the genotypes studied (ANOVA, $F_{(1,178)}$=0.08, P = 0.779) (Table 4, Supplementary Fig. S2C).

DISCUSSION

Xcm infection in banana stimulates production of callose and H_2O_2

In this study, we examined the *Xcm*-mediated callose deposition and H_2O_2 production as early defense signals in BXW and demonstrated for the first-time striking variations between vegetative organs of the banana plants. Furthermore, these differences were independent of resistant or susceptible genotypes. A previous study showed that resistance to BXW in *M.*

balbisiana is not due to hypersensitive response, systemic acquired resistance or induced systemic resistance (Ssekiwoko et al., 2015). However, another study showed that *Xcm*-mediated up-regulation of biotic stress related genes was higher in *M. balbisiana* than in the BXW-susceptible Kayinja (Tripathi et al., 2019) indicating activation of both PTI and ETI. Our findings described here show that callose and H_2O_2 are physiological signatures of PTI in banana-*Xcm* interaction.

Callose was present in banana tissues prior to inoculation because besides plant immunity, callose is widely distributed naturally and participates in numerous biological processes in plants such as development and plasmodesmata function (Piršelová et al., 2012; Nedukha, 2015; Schneider et al., 2016). The increase in *Xcm*-mediated callose deposition suggests the central significance of callose in defense against *Xcm* in bananas. Similarly, a rapid increase in H_2O_2 suggests an oxidative burst as one of the earliest responses in banana defense against *Xcm*. Previous studies in bananas (e.g. De Ascensao & Dubery, 2000; Van Den Berg et al., 2007) reported no change in callose deposition in either tolerant banana cv. Goldfinger or susceptible cv. Williams challenged with *Fusarium oxysporum* f. sp. *cubense*. Instead, tolerance was associated with induction of cell wall-associated phenolic compounds (De Ascensao & Dubery, 2000; Van Den Berg et al., 2007). In contrast, callose is required for resistance to *X. campestris* pv *campestris* (*Xcc*) and xanthan induces susceptibility in *Nicotiana benthamiana* and *Arabidopsis* by suppressing the callose deposition (Yun et al., 2006). In pepper, strong accumulation of callose and H_2O_2 were detected upon infection with *X. campestris* pv. *vesicatoria* (*Xcv*) deficient in *XopB* type-3 effector protein that is known to interfere with these responses (Üstün et al., 2013; Priller et al., 2016). Furthermore, *X. citri* pv. *citri* (*Xcc*) using its HrpE protein (which is a component of the type III secretion system) triggers defense responses in host and non-host plants that include callose deposition, H_2O_2

548 production and other responses (Gottig et al., 2018). The drop in H_2O_2 production shown in
549 our study at 6 hpi could be explained by the activity of H_2O_2 scavenging enzymes such as
550 superoxide dismutase, ascorbate peroxidase and catalase (Gambino et al., 2013; Kreslavski et
551 al., 2013). The biphasic H_2O_2 production observed in our study was similar to Cui et al.
552 (2019) in which H_2O_2 was produced in a biphasic manner in the xylem tissues of wounded
553 *Dalbergia odorifera* stems, with the first peak at 2 hpi, followed by a drop at 6 hpi and a
554 second peak at 12 hpi; then a further drop at 24 hpi. Similarly, Edreva et al. (2015) observed
555 a biphasic production of H_2O_2 in UV-B irradiated cell suspension cultures of the green
556 microalga *Chlorella vulgaris* with the first peak at 30 min- and second peak at 4 hours-post
557 exposure. They propose that the first peak could have signal functions while the second one
558 that is longer and more sustained could be playing a vital role in initiation of PCD (Edreva et
559 al., 2015). Biphasic production of H_2O_2 in plant defense against biotic and abiotic stress have
560 also been reported elsewhere (Wi et al., 2012; Pellegrini et al., 2013; Castro et al., 2021).
561 Callose production peaking at between 14 and 28 dpi followed by a progressive decline in the
562 different organs is consistent with the time needed for appearance of BXW symptoms at 11-
563 21 dpi as observed under this study and previously under field conditions (Tushemereirwe et
564 al., 2004; Smith et al., 2008), suggesting possible correlations between onset of symptoms
565 and decline in callose production. Similarly, decline in callose depositions coinciding with
566 the onset of symptoms were previously observed in pepper infected with *Xcv* (Priller et al.,
567 2016) and tomato infected with *Pseudomonas syringe* (Popov et al., 2016).
568

569 **Vegetative organs of banana vary in their *Xcm*-mediated responses**

570 The banana organs showed differences in responses to infection, suggesting variable abilities
571 of different organs in banana response to *Xcm*. This was surprising because pathogen-induced
572 callose deposition is known to be localized to callosic papillae, providing strategic structural

defense against pathogens and providing targeted delivery of chemical defenses at the sites of pathogen attack (Chowdhury et al., 2014; Ellinger & Voigt, 2014; Schneider et al., 2016; Kashyap et al., 2020). Similarly, H_2O_2 activates antimicrobial defenses at or near sites of infection stimulating HR to limit pathogens to the infection site (Torres et al., 2006; Jambunathan, 2010; Bigeard et al., 2015). We therefore anticipated highest callose deposition in the aerial banana organs such as leaves and pseudostems since *Xcm* naturally gains entry via the aerial tissues. However, this was not the case. Our results showed highest *Xcm*-mediated callose in corms indicating that the corm may be the main organ of *Xcm*-mediated callose-based defenses. In contrast, highest *Xcm*-mediated H_2O_2 was shown in the pseudostem. These findings suggest organ-based defense responses against *Xcm* or organ-specific determinants of resistance / susceptibility similar to what was previously observed in other pathosystems (Lyons et al., 2015; Park & Ryu, 2015; Strugala et al., 2015; Song et al., 2016; Chuberre et al., 2018). For example, defense mechanisms against some pathogenic fungi differ in roots and leaves of the same plant (Heath, 1991; Jansen et al., 2006; Strugala et al., 2015). In maize, roots show a stronger defense response than leaves upon shoot inoculation with *Colletotrichum graminicola* (Balmer et al., 2013). Similarly, strong differences in callose expression and callose synthese activities were observed in stem, leaf blade and spike tissues of wheat suggesting organ-specific expressions patterns (Voigt et al., 2006). Leaves and tubers of potato (*Solanum tuberosum*) activate contrasting defense responses in terms of ROS production and activation of defense genes following treatments with *Phytopthora* PAMP Pep-25 or bacterial PAMP flg22, indicating organ-specific responses to PAMPs (Lacaze & Joly, 2021). Although most of these organ-specific defenses are in response to phytopathogenic fungi and in relatively smaller plants compared to bananas, it seems reasonable that organ-specific responses observed in the current study are more of a rule than an exception.

598

599 **The corm is essential in *Xcm*-mediated responses in banana**

600 The banana corm is a subterranean modified stem, provides attachment for the roots and
601 serves as an organ of perennation supporting vegetative and perennial continuity of the crop
602 across seasons and in this sense, its active participation ensuring a disease-free next
603 generation should be a relevant feature. Plants on the same "mat" are anatomically connected
604 with each other via the corm (Skutch, 1932; Robinson & Galán Saúco, 2010) in which *Xcm*-
605 mediated defenses under this study may be viewed as a form "mother-to-offspring"
606 transmission bottleneck against *Xcm* into lateral shoots. Generally, growth and developmental
607 programs of plants are constrained by tradeoffs with defense against pathogens depending on
608 what is most essential at a given time (Huot et al., 2014; Smakowska et al., 2016; Karasov et
609 al., 2017). Therefore, a BXW-infested mother plant on the corm may be sacrificed at the
610 expense of *Xcm*-mediated defense for healthy or latently infected lateral shoots. As such,
611 incomplete systemic movement of *Xcm* in mats coupled to a gradual decline of bacterial load
612 in subsequent generations to levels that cannot initiate (or take very long, 5-16 months to
613 initiate) disease have been observed (Ocimati et al., 2013; Ocimati et al., 2015). We observed
614 the characteristic orange-yellowish bacterial ooze from the cut surfaces of corms of
615 inoculated plants of Kayinja and Mbwazirume (*data not shown*) but did not test for *Xcm* in
616 those tissues. Our expectation is that bacterial invasion into the corm should be relatively low
617 because of leaf- and pseudostem-based defense barriers mounted prior to entry into the corm.
618 Also, mother banana plants can be 3 to 6 meters tall (Skutch, 1932; Robinson & Galán Saúco,
619 2010); the distal location of the corm with respect to leaves as entry points for the bacteria
620 may provide an "anatomical leverage" for the plant to assemble defenses in the corm and/or
621 escape the infection of the lateral shoots. Previously, no diseased plants were observed in
622 corm-inoculated Mbwazirume plants and for Kayinja, only 1-15% of mild symptom

incidences were observed along the true stem and fruit of some plants (Nakato et al., 2014). This study found no significant differences between the control and the corm inoculation for all symptoms compared to inoculations made in other tissues. In contrast, flower-inoculated plants show fast *Xcm* movement through the true stem to the leaf sheaths and corm of the mother plants and from where the bacteria invade the corm and the pseudostem of the attached suckers (Ssekiwoko et al., 2006a). It is plausible that *Xcm*-mediated defenses observed in our study promote attenuation of *Xcm* progression from leaves which constrains bacterial entry from the pseudostem into younger lateral shoots via the corm; hence, the entire plant in susceptible varieties is sacrificed at the expense of the lateral shoots on the same mat. Whether or not faster disease development and/or defense responses may arise from flower- than leaf-inoculations of *Xcm* in bananas is an interesting future topic to study. Thus, in early stages of infection, the bacteria are restricted to the upper parts of the true stem (Ssekiwoko et al., 2006a) (and pseudostem) and these allow successful SDSR for BXW management in which diseased banana stems are aseptically removed at the soil (or corm) level immediately after observation of leaf or fruit symptoms (Kubiriba et al., 2014).

Xcm-mediated callose and H_2O_2 alone do not account for resistance to BXW

Although all the banana genotypes grown in ECA are susceptible and succumb to BXW once infected (Ssekiwoko et al., 2006b; Tripathi et al., 2008; Ssekiwoko et al., 2013; Nakato et al., 2019), previous observations show that Kayinja is relatively more susceptible than Mbwazirume (Ssekiwoko et al., 2006b; Tripathi et al., 2008; Nakato et al., 2019). This differential susceptibility was also observed under our study because Kayinja plants succumbed to BXW faster than Mbwazirume. However, no significant differences in H_2O_2 production were found between susceptible and resistant genotypes under this study, suggesting that these responses alone may not account for the observed differential

susceptibilities between these genotypes. Moreover, the results were unexpected for *M. balbisiana* (analyzed only for callose deposition under this study) because this genotype is resistant to BXW (Ssekiwoko et al., 2006b; Tripathi et al., 2008; Ssekiwoko et al., 2013; Nakato et al., 2019), however, under this study, it could not be differentiated from susceptible genotypes by the ELISA method. The observed difference between ELISA and fluorescence microscopy results for callose quantification in the genotypes could have been due to sensitivity of the two methods because ELISA is prone to false positives and may have less discriminating power. While *Xcm* disables host detection systems and related downstream reactions both in resistant and susceptible genotypes, the bacteria fail to establish in *M. balbisiana* where its multiplication and migration was slowed and subsequently cleared from host tissues (Ssekiwoko et al., 2013; Ssekiwoko et al., 2015). A recent study showed that many of differentially expressed genes (DEGs) (that mapped to the biotic stress pathways) were higher in *M. balbisiana* than Kayinja, suggesting activation of early response to *Xcm* infection via both PTI and ETI in *M. balbisiana* (Tripathi et al., 2019). These authors further observed suppression of most genes associated with β-1,3-glucanases that degrade callose to ensure callose accumulation in *M. balbisiana* after inoculation with *Xcm* at 12 hpi, suggesting cell wall enforcement by callose deposition. Pathogen-derived callose deposition is one of the early defense "hallmarks" in plants against pathogens (Voigt, 2014; Wang et al., 2021). Our results indicate that although a substantial amount of callose deposition occurs in response to *Xcm* infection, callose alone may not account for BXW resistance in *M. balbisiana.* Even though the fluorescence microscopy results showed that there was significant callose production between *M. balbisiana* and Kayinja, this was not the case with Mbwazirume while ELISA method showed no significant variation in callose production between all the three genotypes. Also, neither hypersensitive response, nor systemic acquired resistance or induced systemic resistance accounts for the resistance for *M. balbisiana* against

673 *Xanthomonas vasicola* pv. *musacearum* (*Xvm*, alias *Xcm*) because the bacteria suppress key
674 genes in these pathways (Ssekiwoko et al., 2013; Ssekiwoko et al., 2015). Therefore, other
675 yet to be identified processes could promote resistance in *M. balbisiana*. One possibility is
676 that there are numerous interactions between PTI pathways such that callose deposition
677 becomes part of the complex network culminating into resistance in *M. balbisiana*. For
678 example, *powdery mildew resistant 4* (*pmr4*), a mutant lacking pathogen-induced callose is
679 resistant to pathogens, rather than more susceptible because *pmr4* mutant was associated with
680 hyper-activation of salicylic acid signaling, leading to increased resistance in *Arabidopsis*
681 (Nishimura et al., 2003). Similar observations have been made in tomatoes (Huibers et al.,
682 2013; Santillán Martínez et al., 2020). Also, tolerance of banana to fusarium wilt was linked
683 to significantly increased induction of cell wall-associated phenolic compounds (Van Den
684 Berg et al., 2007). Defense responses of resistant and susceptible banana cultivars treated
685 with biological control agents and *Fusarium oxysporum* f. sp. *cubense* (Foc) were regulated
686 by DEGs in numerous categories of defense pathways (Kaushal et al., 2021). According to
687 Ssekiwoko et al. (2013), *M. balbisiana* resists *Xcm* by slowing the multiplication and
688 migration of the bacterium followed by subsequent death of the affected organs together with
689 the *Xcm* there, which accounts for delayed symptoms and later recovery. Indeed, the
690 assembly of different physico-chemical or structural barriers to pathogen migration is a
691 hallmark for vascular wilt pathogens intended to limit the pathogen spread to distant tissues
692 (Beckman et al., 1982; Robb et al., 1991; Schneider et al., 2016; Pouzoulet et al., 2017; Lee
693 et al., 2019; Kashyap et al., 2020; Planas-Marquès et al., 2020; Sebastià et al., 2021). Such
694 physico-chemical / structural barriers may include a myriad of phenolic compounds, lignin,
695 suberin, tyloses, gels, and callose. In *Solanum dulcamara* a reservoir host for *Ralstonia*
696 *solanacearum*, resistance to the bacterial wilt is due to restricted colonization of the bacteria
697 (Sebastià et al., 2021). It is reasonable that *Xcm* resistance in *M. balbisiana* may be a multi-

component strategy curtailing the multiplication and migration of bacteria, the dissection of which will benefit from future studies.

Detectability of callose in roots by fluorescence microscopy and ELISA methods

Callose deposition was determined under this study using two independent methods; fluorescence microscopy and ELISA (Piršelová & Matušíková, 2013) and these were applied for the first time to bananas. Fluorescence microscopy is a well-established based on staining with aniline which forms fluorescing complexes (Stone et al., 1984). In contrast, the ELISA method which is not well-stablished is based on enzyme immunoassay (EIA) used to detect the presence of an antigen/ligand (in this case, callose) in the crude 1M NaOH banana extract using antibodies directed against callose (Engvall & Perlmann, 1971; Van Weemen & Schuurs, 1971; Anderson & McNellis, 1998). While a few differences were observed in the data (e.g., the peaking of callose deposits in the different tissues), statistical analysis largely showed congruence of fluorescence microscopy and ELISA data, indicating consistency in the two methods of callose detection. However, we highlight that ELISA is highly prone to false positives (Anderson & McNellis, 1998; Hosseini et al., 2018) and may be less reliable than the well-established aniline blue staining and direct observations of callose. For example, no fluorescing callose particles were observed in the root tissues under fluorescent microscopy method. We first viewed this to imply that banana roots are irrelevant with respect to *Xcm*-mediated defense but ELISA provided contradictory results, indicating the abundance of *Xcm*-mediated callose in the banana roots. Indeed, both constitutive and pathogen-mediated callose deposits can be found in roots of plant species (Bonhoff et al., 1987; Daayf et al., 1997) although root callose may also arise from soil-borne heavy metal contamination (Wissemeier et al., 1992; Tahara et al., 2005; Piršelová et al., 2012; Nedukha, 2015; Zhang et al., 2015). Indeed, the discrepancy between aniline blue staining and ELISA

may be accounted for by the fact that ELISA is prone to false positives and requires further analysis including studies of the physico-chemical properties and anatomical assembly of banana tissues. One possibility is that callose in the roots of banana might occur in "isoforms" that do not easily form complexes with aniline blue compared to the "isoforms" that exist in the other tissues although both types may be easily detectable by ELISA. For example, while most of the callose is characterized by (1,3)-β-branches, some (1,6)-β-branches also occur (Aspinall & Kessler, 1957; Stone & Clarke, 1992; Chen & Kim, 2009) and these could account for variances in biochemistry and/or detectability by different methods. Such is the case in a laticiferous plant, *Euphorbia heterophylla*, in which laticifer walls differ from those of their surrounding cells in that the level of a (1→4)β-D-galactan epitope is much lower in laticifers than in other cells (Serpe et al., 2004). Consequently, an anti-(1→3)β-D-glucan antibody that recognizes callose failed to label laticifer walls and those walls immediately adjacent to laticifers, but it produced a punctuated labeling pattern in most other cells (Serpe et al., 2004). The second possibility is that different plant tissues may accumulate various primary or secondary metabolites, which at higher concentrations may obscure or interfere with fluorescent signal in aniline staining measurement (Smith & McCully, 1978; Ko & Lin, 2004; Piršelová & Matušíková, 2013; Yan et al., 2015). Up to eight glucan synthase-like genes control callose synthesis and are regulated in an organ-specific manner in wheat (Voigt et al., 2006) while at least nine callose synthase genes in stinging nettle (*Urtica dioica*) show variable expression in roots and leaves (Guerriero et al., 2020). However, whether or not the differential controls in synthesis may generate different "forms" of callose or its complexes is unknown. The third possibility is that the various primary or secondary metabolites at higher concentrations in banana roots provide high background noise and with less discriminating power of ELISA may generate false positives of callose in root extracts. Overall, whereas results from the two methods were largely

congruent, it is reasonable that the results from ELISA be interpreted with caution, as the method still requires extensive optimization.

CONCLUSION

Overall, this is the first study to examine pathogen-mediated callose and H_2O_2 production at different tissue and organ levels in response to *Xcm* in bananas and the resulting BXW disease. Our findings point to an organ-specific response to *Xcm* infection in bananas that is independent of resistant or susceptible genotypes. Determination of callose deposits both qualitatively and quantitatively provided fair reproducibility of the data. Although *M. balbisiana* is resistant to *Xcm*, it has not been possible to transfer the resistance to commercial banana cultivars to control BXW, partly because of the challenges associated with its introgression and the resistance mechanism is also not well understood. Effective transgenic resistance against BXW in bananas is available; however, it suffers legislative impediments in the ECA region. Consequently, cultural methods have been used in the management of BXW e.g., SDSR in which only the BXW-diseased plant is removed from the corm while leaving the other symptomless lateral shoots. Pseudostems of infected plants accumulate high quantities of H_2O_2. Our findings that corm accumulates higher quantities of callose (and also H_2O_2) while also supporting a H_2O_2-loaded pseudostem provide a possible mechanistic basis by which *Xcm* progression into lateral shoots is slowed during natural infection. Therefore, corm plays an important role in *Xcm*-mediated response to BXW. It is noteworthy that banana corm is a subterranean organ of perennation allowing perennial continuity of the crop seasons and in this sense, active participation to ensure disease-free next generation should be a desirable and relevant feature. Additional evidence is needed to determine whether or not *Xcm*-medicated callose in the corm may be essential in limiting vertical transmission of *Xcm* into lateral shoots and whether this represents an example of tradeoffs between plant

development and defense against pathogens. Contrary to our expectations, susceptible and resistant genotypes under this study showed no significant differences in relation to levels of *Xcm*-derived callose and H_2O_2, indicating that these are not the primary responses that impart resistance to BXW in *M. balbisiana*. Future studies should be aimed at uncovering other defense responses in *M. balbisiana* that promote resistance against BXW. Furthermore, strategies that increase callose and H_2O_2 production in susceptible bananas without compromising yield could be a potential avenue for controlling BXW in the field.

ACKNOWLEDGEMENTS

We are grateful to Aleš Soukup (Department of Plant Experimental Biology, Charles University in Prague, Czech Republic) for his technical assistance and helpful discussions on this study, and Mark P. Simmons (Colorado State University, USA) for constructive comments on this study. We thank the anonymous reviewers whose constructive criticisms improved the manuscript.

LITERATURE CITED

Abele, S., Twine, E. and Legg, C. (2007). Food Security in Eastern Africa and the Great Lakes *Crop Crisis Control Project (C3P)*: USAID.

Adriko, J., Aritua, V., Mortensen, C. N., Tushemereirwe, W. K., Kubiriba, J. and Lund, O. S. (2012). Multiplex PCR for specific and robust detection of *Xanthomonas campestris* pv. *musacearum* in pure culture and infected plant material. *Plant Pathology, 61*(3), 489-497. doi: https://doi.org/10.1111/j.1365-3059.2011.02534.x

Altenbach, D. and Robatzek, S. (2007). Pattern recognition receptors: from the cell surface to intracellular dynamics. *Molecular Plant-Microbe Interactions, 20*(9), 1031-1039. doi: https://doi.org/10.1094/mpmi-20-9-1031

798 Anderson, G. L. and McNellis, L. A. (1998). Enzyme-linked antibodies: A laboratory
799 introduction to the ELISA assay. *Journal of Chemical Education, 75*(10), 1275. doi:
800 https://doi.org/10.1021/ed075p1275
801 Anderson, J. P., Gleason, C. A., Foley, R. C., Thrall, P. H., Burdon, J. B. and Singh, K. B.
802 (2010). Plants versus pathogens: An evolutionary arms race. *Functional Plant*
803 *Biology, 37*(6), 499-512. doi: https://doi.org/10.1071/FP09304
804 Aspinall, G. O. and Kessler, G. (1957). The structure of callose from the grape vine
805 *Chemistry and Industry*.
806 Balmer, D., de Papajewski, D. V., Planchamp, C., Glauser, G. and Mauch-Mani, B. (2013).
807 Induced resistance in maize is based on organ-specific defence responses. *The Plant*
808 *Journal, 74*(2), 213-225. doi: https://doi.org/10.1111/tpj.12114
809 Beckman, C. H., Mueller, W. C., Tessier, B. J. and Harrison, N. A. (1982). Recognition and
810 callose deposition in response to vascular infection in Fusarium wilt-resistant or
811 susceptible tomato plants. *Physiological Plant Pathology, 20*, 1-10. doi:
812 https://doi.org/10.1016/0048-4059(82)90018
813 Beer. (1852). Bestimmung der Absorption des rothen Lichts in farbigen Flüssigkeiten.
814 *Annalen der Physik, 162*(5), 78-88. doi: https://doi.org/10.1002/andp.18521620505
815 Bigeard, J., Colcombet, J. and Hirt, H. (2015). Signaling mechanisms in pattern-triggered
816 immunity (PTI). *Molecular Plant, 8*, 521–539. doi:
817 https://doi.org/10.1016/j.molp.2014.12.022
818 Blomme, G., Ocimati, W., Sivirihauma, C., Vutseme, L., Mariamu, B., Kamira, M., van
819 Schagen, B., Ekboir, J. and Ntamwira, J. (2017). A control package revolving around
820 the removal of single diseased banana stems is effective for the restoration of
821 Xanthomonas wilt infected fields. *European Journal of Plant Pathology*, 1-16. doi:
822 https://doi.org/10.1007/s10658-017-1189-6

823 Bonhoff, A., Rieth, B., Golecki, J. and Grisebach, H. (1987). Race cultivar-specific
824 differences in callose deposition in soybean roots following infection with
825 *Phytophthora megasperma* f.sp. *glycinea*. *Planta, 172*(1), 101-105. doi:
826 https://doi.org/10.1007/BF00403034
827 Castro, B., Citterico, M., Kimura, S., Stevens, D. M., Wrzaczek, M. and Coaker, G. (2021).
828 Stress-induced reactive oxygen species compartmentalization, perception and
829 signalling. *Nature Plants, 7*(4), 403-412. doi: https://doi.org/10.1038/s41477-021-
830 00887-0
831 Chen, X.-Y. and Kim, J.-Y. (2009). Callose synthesis in higher plants. *Plant signaling &*
832 *behavior, 4*(6), 489-492. doi: https://doi.org/10.4161/psb.4.6.8359
833 Chowdhury, J., Henderson, M., Schweizer, P., Burton, R. A., Fincher, G. B. and Little, A.
834 (2014). Differential accumulation of callose, arabinoxylan and cellulose in
835 nonpenetrated versus penetrated papillae on leaves of barley infected with *Blumeria*
836 *graminis* f. sp. *hordei*. *New Phytol, 204*(3), 650-660. doi:
837 https://doi.org/10.1111/nph.12974
838 Chuberre, C., Plancot, B., Driouich, A., Moore, J. P., Bardor, M., Gügi, B. and Vicré, M.
839 (2018). Plant immunity is compartmentalized and specialized in roots. *Frontiers in*
840 *Plant Science, 9*(1692), 1-13. doi: https://doi.org/10.3389/fpls.2018.01692
841 Cohen, Y., Eyal, H. and Hanania, J. (1990). Ultrastructure, autofluorescence, callose
842 deposition and lignification in susceptible and resistant muskmelon leaves infected
843 with the powdery mildew fungus *Sphaerotheca fuliginea*. *Physiological and*
844 *Molecular Plant Pathology, 36*, 191-204. doi: https://doi.org/10.1016/0885-
845 5765(90)90025-S
846 Cui, Z., Yang, Z. and Xu, D. (2019). Synergistic roles of biphasic ethylene and hydrogen
847 peroxide in wound-induced vessel occlusions and essential oil accumulation in

dalbergia odorifera. *Frontiers in Plant Science, 10*(250). doi: https://doi.org/10.3389/fpls.2019.00250

Daayf, F., Nicole, M., Boher, B., Pando, A. and Geiger, J. P. (1997). Early vascular defense reactions of cotton roots infected with a defoliating mutant strain of *Verticillium dahliae*. *European Journal of Plant Pathology, 103*(2), 125-136. doi: https://doi.org/10.1023/A:1008620410471

Daudi, A. and O'Brien, J. A. (2012). Detection of hydrogen peroxide by DAB staining in *Arabidopsis* leaves. *Bio-protocol, 2*(18). doi: https://doi.org/10.21769/BioProtoc.263

De Ascensao, A. R. and Dubery, I. A. (2000). Panama disease: Cell wall reinforcement in banana roots in response to elicitors from *Fusarium oxysporum* f. sp. *cubense* race four. *Phytopathology, 90*(10), 1173-1180. doi: https://doi.org/10.1094/phyto.2000.90.10.1173

Dodds, P. N. and Rathjen, J. P. (2010). Plant immunity: towards an integrated view of plant-pathogen interactions. *Nature Review Genetics, 11*(8), 539-548. doi: https://doi.org/10.1038/nrg2812

Dotto, J. M., Matemu, A. and Ndakidemi, P. (2018). Potential of cooking bananas in addressing food security in East Africa. *International Journal of Biosciences 13*(4), 278-294. doi: http://doi.org/10.12692/ijb/13.4.278-294

Edreva, A. M., Pouneva, I. D. and Gesheva, E. Z. (2015). UV-B radiation induces biphasic burst of hydrogen peroxide in mesophyll *Chlorella vulgaris*. *Russian Journal of Plant Physiology, 62*(2), 219-223. doi: https://doi.org/10.1134/S1021443715010069

Ellinger, D. and Voigt, C. A. (2014). Callose biosynthesis in arabidopsis with a focus on pathogen response: What we have learned within the last decade. *Annals of Botany, 114*(6), 1349-1358. doi: https://doi.org/10.1093/aob/mcu120

872 Engvall, E. and Perlmann, P. (1971). Enzyme-linked immunosorbent assay (ELISA).
873 Quantitative assay of immunoglobulin G. *Immunochemistry, 8*(9), 871-874. doi:
874 https://doi.org/10.1016/0019-2791(71)90454-x
875 FAOSTAT. (2017). Retrieved Accessed 06 June, 2021 http://www.fao.org/faostat/en/#home
876 Gambino, G., Boccacci, P., Margaria, P., Palmano, S. and Gribaudo, I. (2013). Hydrogen
877 peroxide accumulation and transcriptional changes in grapevines recovered from
878 Flavescence dorée disease. *Phytopathology, 103*(8), 776-784. doi:
879 http://dx.doi.org/10.1094/PHYTO-11-12-0309-R
880 Games, P. A. and Howell, J. F. (1976). Pairwise multiple comparison procedures with
881 unequal N's and/or variances: A Monte Carlo study. *Journal of Educational Statistics,*
882 *1*(2), 113-125. doi: https://doi.org/10.3102/10769986001002113
883 Gottig, N., Vranych, C. V., Sgro, G. G., Piazza, A. and Ottado, J. (2018). HrpE, the major
884 component of the Xanthomonas type three protein secretion pilus, elicits plant
885 immunity responses. *Scientific Reports, 8*(1), 9842. doi:
886 https://doi.org/10.1038/s41598-018-27869-1
887 Guerriero, G., Piasecki, E., Berni, R., Xu, X., Legay, S. and Hausman, J.-F. (2020).
888 Identification of callose synthases in stinging nettle and analysis of their expression in
889 different tissues. *International Journal of Molecular Sciences, 21*(11), 3853. doi:
890 https://doi.org/10.3390/ijms21113853
891 Heath, M. C. (1991). Evolution of resistance to fungal parasitism in natural ecosystems. *New*
892 *Phytologist, 119*(3), 331-343. doi: https://doi.org/10.1111/j.1469-
893 8137.1991.tb00034.x
894 Hosseini, S., Vázquez-Villegas, P., Rito-Palomares, M. and Martinez-Chapa, S. O. (2018).
895 *Enzyme-Linked Immunosorbent Assay (ELISA) From A to Z*. Singapore 189721,
896 Singapore: Springer Nature.

Huibers, R. P., Loonen, A. E. H. M., Gao, D., Van den Ackerveken, G., Visser, R. G. F. and Bai, Y. (2013). Powdery mildew resistance in tomato by impairment of *SLPMR4* and *SLDMR1*. *PLOS ONE, 8*(6), e67467. doi: https://doi.org/10.1371/journal.pone.0067467

Huot, B., Yao, J., Montgomery, B. L. and He, S. Y. (2014). Growth-defense tradeoffs in plants: a balancing act to optimize fitness. *Molecular plant, 7*(8), 1267-1287. doi: https://doi.org/10.1093/mp/ssu049

Jambunathan, N. (2010). Determination and detection of reactive oxygen species (ROS), lipid peroxidation, and electrolyte leakage in plants. In R. Sunkar (Ed.), *Plant Stress Tolerance: Methods and Protocols* (pp. 291-297). Totowa, NJ: Humana Press.

Jansen, M., Slusarenko, A. J. and Schaffrath, U. (2006). Competence of roots for race-specific resistance and the induction of acquired resistance against *Magnaporthe oryzae*. *Molecular Plant Pathology, 7*(3), 191-195. doi: https://doi.org/10.1111/j.1364-3703.2006.00331.x

Jones, J. D. G. and Dangl, J. L. (2006). The plant immune system. *Nature, 444*, 323-329. doi: https://doi.org/10.1038/nature05286

Karasov, T. L., Chae, E., Herman, J. J. and Bergelson, J. (2017). Mechanisms to mitigate the trade-off between growth and defense. *The Plant Cell, 29*(4), 666-680. doi: https://doi.org/10.1105/tpc.16.00931

Kashyap, A., Planas-Marquès, M., Capellades, M., Valls, M. and Coll, N. S. (2020). Blocking intruders: inducible physico-chemical barriers against plant vascular wilt pathogens. *Journal of experimental botany, 72*(2), 184-198. doi: https://doi.org/10.1093/jxb/eraa444

Kaushal, M., Mahuku, G. and Swennen, R. (2021). Comparative transcriptome and expression profiling of resistant and susceptible banana cultivars during infection by

Fusarium oxysporum. *International Journal of Molecular Sciences, 22*(6). doi: https://doi.org/10.3390/ijms22063002

Khaledi, N., Taheri, P. and Falahati-Rastegar, M. (2018). Evaluation of resistance and the role of some defense responses in wheat cultivars to Fusarium head blight. *Journal of Plant Protection Research, 0*(0). doi: https://doi.org/10.1515/jppr-2017-0054

Ko, Y. T. and Lin, Y. L. (2004). 1,3-beta-glucan quantification by a fluorescence microassay and analysis of its distribution in foods. *Journal of Agricultural and Food Chemistry, 52*(11), 3313-3318. doi: https://doi.org/10.1021/jf0354085

Kohari, M., Yashima, K., Desaki, Y. and Shibuya, N. (2016). Quantification of stimulus-induced callose spots on plant materials. *Plant Biotechnology, 33*, 11-17. doi: https://doi.org/10.5511/plantbiotechnology.15.1120a

Kohler, A., Schwindling, S. and Conrath, U. (2000). Extraction and quantitative determination of callose from Arabidopsis leaves. *BioTechniques, 28*, 1084-1086.

Kreslavski, V. D., Lyubimov, V. Y., Shirshikova, G. N., Shmarev, A. N., Kosobryukhov, A. A., Schmitt, F.-J., Friedrich, T. and Allakhverdiev, S. I. (2013). Preillumination of lettuce seedlings with red light enhances the resistance of photosynthetic apparatus to UV-A. *Journal of Photochemistry and Photobiology B: Biology, 122*, 1-6. doi: https://doi.org/10.1016/j.jphotobiol.2013.02.016

Kubiriba, J., Muthomi, J., Ndungo, V., Kwach, J., Erima, R., Rwomushana, I., Tushemereirwe, W. and Opio, F. (2014). Strategies for rehabilitation of banana fields infested with *Xanthomonas campestris* pv. *musacearum*. *Journal of Crop Protection, 3*(1), 21-29. doi: http://jcp.modares.ac.ir/article-3-2426-en.html

Kuźniak, E. and Urbanek, H. (2000). The involvement of hydrogen peroxide in plant responses to stresses. *Acta Physiologiae Plantarum, 22*(2), 195-203. doi: https://doi.org/10.1007/s11738-000-0076-4

947 Lacaze, A. and Joly, D. L. (2021). Leaf and tuber treatments with PAMPs trigger organ-
948 specific responses in potato. *Canadian Journal of Plant Pathology*, 1-13. doi:
949 https://doi.org/10.1080/07060661.2021.1969595
950 Lambert, J. H. (1760). Photometria sive de mensura et gradibus luminis, colorum et umbrae
951 [Photometry, or, On the measure and gradations of light intensity, colors, and shade]
952 Lee, M.-H., Jeon, H. S., Kim, S. H., Chung, J. H., Roppolo, D., Lee, H.-J., Cho, H. J.,
953 Tobimatsu, Y., Ralph, J. and Park, O. K. (2019). Lignin-based barrier restricts
954 pathogens to the infection site and confers resistance in plants. *The EMBO Journal,*
955 *38*(23), e101948. doi: https://doi.org/10.15252/embj.2019101948
956 Luna, E., Pastor, V., Robert, J., Flors, V., Mauch-Mani, B. and Ton, J. (2011). Callose
957 deposition: A multifaceted plant defense response. *The American Phytopathological*
958 *Society, 24*(2), 183-193. doi: https://doi.org/10.1094/MPMI-07-10-0149
959 Lyons, R., Stiller, J., Powell, J., Rusu, A., Manners, J. M. and Kazan, K. (2015). *Fusarium*
960 *oxysporum* triggers tissue-specific transcriptional reprogramming in *Arabidopsis*
961 *thaliana*. *PLOS ONE, 10*(4), e0121902. doi:
962 https://doi.org/10.1371/journal.pone.0121902
963 Malinovsky, F. G., Fangel, J. U. and Willats, W. G. T. (2014). The role of the cell wall in
964 plant immunity. *Frontiers in Plant Science, 5*(178). doi:
965 https://doi.org/10.3389/fpls.2014.00178
966 Moore, J. W., Loake, G. J. and Spoel, S. H. (2011). Transcription Dynamics in Plant
967 Immunity. *The Plant Cell, 23*(8), 2809-2820. doi:
968 https://doi.org/10.1105/tpc.111.087346
969 Mwangi, M., Bandyopadhyay, R., Ragama, P. and Tushemereirwe, W. K. (2007).
970 Assessment of banana planting practices and cultivar tolerance in relation to

management of soilborne *Xanthomonas campestris* pv *musacearum*. *Crop Protection, 26*(8), 1203-1208. doi: http://doi.org/10.1016/j.cropro.2006.10.017

Nakato, G. V., Christelová, P., Were, E., Nyine, M., Coutinho, T. A., Doležel, J., Uwimana, B., Swennen, R. and Mahuku, G. (2019). Sources of resistance in Musa to *Xanthomonas campestris* pv. *musacearum*, the causal agent of banana Xanthomonas wilt. *Plant Pathology, 68*(1), 49-59. doi: https://doi.org/10.1111/ppa.12945

Nakato, V., Ocimati, W., Blomme, G., Fiaboe, K. K. M. and Beed, F. (2014). Comparative importance of infection routes for banana Xanthomonas wilt and implications on disease epidemiology and management. *Canadian Journal of Plant Pathology, 36*(4), 418-427. doi: https://doi.org/10.1080/07060661.2014.959059

Nakato, V., Mahuku, G. and Coutinho, T. (2018). *Xanthomonas campestris* pv. *musacearum*: A major constraint to banana, plantain and enset production in central and east Africa over the past decade. *Molecular Plant Pathology, 19*(3), 525-536. doi: https://doi.org/10.1111/mpp.12578

Ndungo, V., Eden-Green, S., Blomme, G., Crozier, J. and Smith, J. J. (2006). Presence of banana Xanthomonas wilt (*Xanthomonas campestris* pv. *musacearum*) in the Democratic Republic of Congo (DRC). *Plant Pathology, 55*(2), 294. doi: https://doi.org/10.1111/j.1365-3059.2005.01258.x

Nedukha, O. (2015). Callose: Localization, functions, and synthesis in plant cells. *Cytology and Genetics, 49*(1), 49-57. doi: https://doi.org/10.3103/S0095452715010090

Nelson, T. E. and Lewis, B. A. (1974). Separation and characterization of the soluble and insoluble components of insoluble laminaran. *Carbohydrate Research, 33*(1), 63-74. doi: https://doi.org/10.1016/s0008-6215(00)82940-7

994 Nicaise, V., Roux, M. and Zipfel, C. (2009). Recent advances in PAMP-triggered immunity
995 against bacteria: Pattern recognition receptors watch over and raise the alarm. *Plant*
996 *Physiology, 150*(4), 1638-1647. doi: https://doi.org/10.1104/pp.109.139709
997 Nishimura, M. T., Stein, M., Hou, B.-H., Vogel, J. P., Edwards, H. and Somerville, S. C.
998 (2003). Loss of a callose synthase results in salicylic acid-dependent disease
999 resistance. *Science, 301*(5635), 969-972. doi: https://doi.org/10.1126/science.1086716
1000 Noctor, G., Lelarge-Trouverie, C. and Mhamdi, A. (2015). The metabolomics of oxidative
1001 stress. *Phytochemistry, 112*, 33-53. doi:
1002 https://doi.org/10.1016/j.phytochem.2014.09.002
1003 O'Brien, J. A., Daudi, A., Butt, V. S. and Bolwell, G. P. (2012). Reactive oxygen species and
1004 their role in plant defence and cell wall metabolism. *Planta, 236*(3), 765-779. doi:
1005 https://doi.org/10.1007/s00425-012-1696-9
1006 Ocimati, W., Ssekiwoko, F., Karamura, E., Tinzaara, W., Eden-Green, S. and Blomme, G.
1007 (2013). Systemicity of *Xanthomonas campestris* pv. *musacearum* and time to disease
1008 expression after inflorescence infection in East African Highland and Pisang Awak
1009 bananas in Uganda. *Plant Pathology, 62*(4), 777-785. doi:
1010 https://doi.org/10.1111/j.1365-3059.2012.02697.x
1011 Ocimati, W., Nakato, G. V., Fiaboe, K. M., Beed, F. and Blomme, G. (2015). Incomplete
1012 systemic movement of *Xanthomonas campestris* pv. *musacearum* and the occurrence
1013 of latent infections in Xanthomonas wilt-infected banana mats. *Plant Pathology, 64*,
1014 81–90. doi: https://doi.org/10.1111/ppa.12233
1015 Ocimati, W., Bouwmeester, H., Groot, J. C. J., Tittonell, P., Brown, D. and Blomme, G.
1016 (2019). The risk posed by Xanthomonas wilt disease of banana: Mapping of disease
1017 hotspots, fronts and vulnerable landscapes. *PLOS ONE, 14*(4), e0213691. doi:
1018 https://doi.org/10.1371/journal.pone.0213691

1019 Park, Y.-S. and Ryu, C.-M. (2015). Inter-organ defense networking: Leaf whitefly sucking
1020 elicits plant immunity to crown gall disease caused by *Agrobacterium tumefaciens*.
1021 *Plant Signaling & Behavior, 10*(11), e1081325. doi:
1022 https://doi.org/10.1080/15592324.2015.1081325
1023 Patterson, B. D., MacRae, E. A. and Ferguson, I. B. (1984). Estimation of hydrogen peroxide
1024 in plant extracts using titanium (IV). *Analytical Biochemistry, 139*(2), 487-492. doi:
1025 https://doi.org/10.1016/0003-2697(84)90039-3
1026 Pellegrini, E., Trivellini, A., Campanella, A., Francini, A., Lorenzini, G., Nali, C. and
1027 Vernieri, P. (2013). Signaling molecules and cell death in *Melissa officinalis* plants
1028 exposed to ozone. *Plant Cell Reports, 32*(12), 1965-1980. doi:
1029 https://doi.org/10.1007/s00299-013-1508-0
1030 Piršelová, B., Mistríková, V., Libantová, J., Moravčíková, J. and Matušíková, I. (2012).
1031 Study on metal-triggered callose deposition in roots of maize and soybean. *Biologia,*
1032 *67*(4), 698-705. doi: https://doi.org/10.2478/s11756-012-0051-8
1033 Piršelová, B. and Matušíková, I. (2013). Callose: the plant cell wall polysaccharide with
1034 multiple biological functions. *Acta Physiologiae Plantarum, 35*(3), 635-644. doi:
1035 https://doi.org/10.1007/s11738-012-1103-y
1036 Planas-Marquès, M., Kressin, J. P., Kashyap, A., Panthee, D. R., Louws, F. J., Coll, N. S. and
1037 Valls, M. (2020). Four bottlenecks restrict colonization and invasion by the pathogen
1038 *Ralstonia solanacearum* in resistant tomato. *Journal of experimental botany, 71*(6),
1039 2157-2171. doi: https://doi.org/10.1093/jxb/erz562
1040 Popov, G., Fraiture, M., Brunner, F. and Sessa, G. (2016). Multiple *Xanthomonas*
1041 *euvesicatoria* Type III effectors inhibit flg22-triggered immunity. *Molecular Plant-*
1042 *Microbe Interactions, 29*(8), 651-660. doi: https://doi.org/10.1094/mpmi-07-16-0137-
1043 r

Pouzoulet, J., Scudiero, E., Schiavon, M. and Rolshausen, P. E. (2017). Xylem vessel diameter affects the compartmentalization of the vascular pathogen *Phaeomoniella chlamydospora* in grapevine. *Frontiers in Plant Science, 8*, 1442. doi: https://doi.org/10.3389/fpls.2017.01442

Priller, J. P. R., Reid, S., Konein, P., Dietrich, P. and Sonnewald, S. (2016). The *Xanthomonas campestris* pv. *vesicatoria* Type-3 Effector XopB inhibits plant defence responses by interfering with ROS production. *PLOS ONE, 11*(7), e0159107. doi: https://doi.org/10.1371/journal.pone.0159107

R Core Team. (2020). R: A language and environment for statistical computing (Version 3.6.3). Vienna, Austria: R Foundation for Statistical Computing. Retrieved from https://www.r-project.org/

Reen, D. J. (1994). Enzyme-Linked Immunosorbent Assay (ELISA). In J. M. Walker (Ed.), *Basic Protein and Peptide Protocols* (pp. 461-466). Totowa, NJ: Humana Press.

Rioux, L. E., Turgeon, S. L. and Beaulieu, M. (2007). Characterization of polysaccharides extracted from brown seaweeds. *Carbohydrate Polymers, 69*(3), 530-537. doi: https://doi.org/10.1016/j.carbpol.2007.01.009

Robb, J., Lee, S.-W., Mohan, R. and Kolattukudy, P. E. (1991). Chemical characterization of stress-induced vascular coating in tomato 1. *Plant Physiology, 97*(2), 528-536. doi: https://doi.org/10.1104/pp.97.2.528

Robinson, J. C. and Galán Saúco, V. (2010). *Bananas and plantains*. Cambridge, USA: MPG Books Group.

Santillán Martínez, M. I., Bracuto, V., Koseoglou, E., Appiano, M., Jacobsen, E., Visser, R. G. F., Wolters, A.-M. A. and Bai, Y. (2020). CRISPR/Cas9-targeted mutagenesis of the tomato susceptibility gene *PMR4* for resistance against powdery mildew. *BMC Plant Biology, 20*(1), 284. doi: https://doi.org/10.1186/s12870-020-02497-y

Schenk, S. T. and Schikora, A. (2015). Staining of callose depositions in root and leaf tissues. *Bio-protocol, 5*(6). doi: https://www.bio-protocol.org/e1429

Schneider, R., Hanak, T., Persson, S. and Voigt, C. A. (2016). Cellulose and callose synthesis and organization in focus, what's new? *Current opinion in plant biology, 34*, 9-16. doi: https://doi.org/10.1016/j.pbi.2016.07.007

Schwessinger, B. and Zipfel, C. (2008). News from the frontline: recent insights into PAMP-triggered immunity in plants. *Current opinion in plant biology, 11*(4), 389-395. doi: https://doi.org/10.1016/j.pbi.2008.06.001

Sebastià, P., de Pedro-Jové, R., Daubech, B., Kashyap, A., Coll, N. S. and Valls, M. (2021). The bacterial wilt reservoir host *Solanum dulcamara* shows resistance to *Ralstonia solanacearum* infection. *Frontiers in Plant Science, 12*(2408). doi: https://doi.org/10.3389/fpls.2021.755708

Serpe, M., Muir, A. J., Andème-Onzighi, C. and Driouich, A. (2004). Differential distribution of callose and a (1→4)β-D-galactan epitope in the laticiferous plant *Euphorbia heterophylla* L. *International Journal of Plant Sciences, 165*(4), 571-585. doi: http://doi.org/10.1086/386563

Skutch, A. F. (1932). Anatomy of the axis of the banana. *Botanical Gazette, 93*(3), 233-258.

Smakowska, E., Kong, J., Busch, W. and Belkhadir, Y. (2016). Organ-specific regulation of growth-defense tradeoffs by plants. *Current opinion in plant biology, 29*, 129-137. doi: https://doi.org/10.1016/j.pbi.2015.12.005

Smith, J. J., Jones, D. R., Karamura, E., Blomme, G. and Turyagyenda, F. L. (2008). An analysis of the risk from *Xanthomonas campestris* pv. *musacearum* to banana cultivation in Eastern, Central and Southern Africa. Montpellier, France: Bioversity International.

Smith, M. M. and McCully, M. E. (1978). A critical evaluation of the specificity of aniline blue induced fluorescence. *Protoplasma, 95*(3), 229-254. doi: https://doi.org/10.1007/BF01294453

Song, G. C., Sim, H.-J., Kim, S.-G. and Ryu, C.-M. (2016). Root-mediated signal transmission of systemic acquired resistance against above-ground and below-ground pathogens. *Annals of Botany, 118*(4), 821-831. doi: https://doi.org/10.1093/aob/mcw152

Soukup, A. and Tylová, E. (2014). Essential methods of plant sample preparation for light microscopy. In V. Žárský and F. Cvrcˇ ková (Eds.), *Plant Cell Morphogenesis: Methods and Protocols, Methods in Molecular Biology* (Vol. 1080). New York: Springer Science+Business Media.

Ssekiwoko, F., Turyagyenda, L. F., Mukasa, H., Eden-Green, S. and Blomme, G. (2006a). Systemicity of *Xanthomonas campestris* pv. *musacearum* in flower-infected banana plants 789-793.

Ssekiwoko, F., Tushemereirwe, W. K., Batte, M., Ragama, P. E. and Kumakech, A. (2006b). Reaction of banana germplasm to inoculum with *Xanthomonas campestris* pv. *musacearum African Crop Science Journal, 14*(2), 151-156.

Ssekiwoko, F., Kunert, K., Kiggundu, A., Tushemereirwe, W. K. and Karamura, E. (2013). *Musa balbisiana* resists *Xanthomonas* wilt disease through interfering with the multiplication of *Xanthomonas vasicola* pv *musacearum* coupled with whole organ (leaf) death. *Uganda Journal of Agricultural Sciences, 14*(2), 13-25.

Ssekiwoko, F., Kiggundu, A., Tushemereirwe, W. K., Karamura, E. and Kunert, K. (2015). *Xanthomonas vasicola* pv. *musacearum* down-regulates selected defense genes during its interaction with both resistant and susceptible banana. *Physiological and*

Molecular Plant Pathology, 90, 21-26. doi: https://doi.org/10.1016/j.pmpp.2015.02.007

Stone, B. A., Evans, N. A., Bonig, I. and Clarke, A. E. (1984). The application of Sirofluor, a chemically defined fluorochrome from aniline blue for the histochemical detection of callose. *Protoplasma, 122*(3), 191-195. doi: https://doi.org/10.1007/BF01281696

Stone, B. A. and Clarke, A. C. (1992). *Chemistry and Biology of (1->3)-b-Glucans*. Bundoora, Victoria: La Trobe University Press.

Strugala, R., Delventhal, R. and Schaffrath, U. (2015). An organ-specific view on non-host resistance. *Frontiers in Plant Science, 6*(526). doi: https://doi.org/10.3389/fpls.2015.00526

Studholme, D. J., Wicker, E., Abrare, S. M., Aspin, A., Bogdanove, A., Broders, K., Dubrow, Z., Grant, M., Jones, J. B., Karamura, G., Lang, J., Leach, J., Mahuku, G., Nakato, G. V., Coutinho, T., Smith, J. and Bull, C. T. (2020). Transfer of *Xanthomonas campestris* pv. *arecae* and *X. campestris* pv. *musacearum* to *X. vasicola* (Vauterin) as *X. vasicola* pv. *arecae* comb. nov. and *X. vasicola* pv. *musacearum* comb. nov. and Description of *X. vasicola* pv. *vasculorum* pv. nov. *Phytopathology®, 110*(6), 1153-1160. doi: https://doi.org/10.1094/phyto-03-19-0098-le

Tahara, K., Norisada, M., Hogetsu, T. and Kojima, K. (2005). Aluminum tolerance and aluminum-induced deposition of callose and lignin in the root tips of *Melaleuca* and *Eucalyptus* species. *Journal of Forest Research, 10*(4), 325-333. doi: https://doi.org/10.1007/s10310-005-0153-z

Torres, M. A., Jones, J. D. G. and Dangl, J. L. (2006). Reactive oxygen species signaling in response to pathogens. *Plant Physiology, 141*(2), 373-378. doi: https://doi.org/10.1104/pp.106.079467

Tripathi, L., Tripathi, J. N., Tushemereirwe, W. K. and Bandyopadhyay, R. (2007). Development of a semi-selective medium for isolation of *Xanthomonas campestris* pv. *musacearum* from banana plants. *European Journal of Plant Pathology, 117*(2), 177-186. doi: https://doi.org/10.1007/s10658-006-9083-7

Tripathi, L., Odipio, J., Tripathi, J. N. and Tusiime, G. (2008). A rapid technique for screening banana cultivars for resistance to Xanthomonas wilt. *European Journal of Plant Pathology, 121*(1), 9-19. doi: https://doi.org/10.1007/s10658-007-9235-4

Tripathi, L., Tripathi, J. N. and Kubiriba, J. (2016). Transgenic technologies for bacterial wilt resistance *Banana: Genomics and transgenic approaches for genetic improvement* (pp. 197-209).

Tripathi, L., Atkinson, H., Roderick, H., Kubiriba, J. and Tripathi, J. N. (2017). Genetically engineered bananas resistant to Xanthomonas wilt disease and nematodes. *Food and energy security, 6*(2), 37-47. doi: https://doi.org/10.1002/fes3.101

Tripathi, L., Tripathi, J. N., Shah, T., Muiruri, K. S. and Katari, M. (2019). Molecular basis of disease resistance in banana progenitor *Musa balbisiana* against *Xanthomonas campestris* pv. *musacearum*. *Scientific Reports, 9*(7007), 1-17. doi: https://doi.org/10.1038/s41598-019-43421-1

Tushemereirwe, W. K., Kangire, A., Ssekiwoko, F., Offord, L. C., Crozier, J., Ba, E., Rutherford, M. and Smith, J. J. (2004). First report of *Xanthomonas campestris* pv. *musacearum* on banana in Uganda. *Plant Pathology, 53*, 802. doi: doi.org/10.1111/j.1365-3059.2004.01090.x

Underwood, W. (2012). The plant cell wall: A dynamic barrier against pathogen invasion. *Frontiers in Plant Science, 3*(85). doi: https://doi.org/10.3389/fpls.2012.00085

Üstün, S., Bartetzko, V. and Börnke, F. (2013). The *Xanthomonas campestris* Type III effector *Xopj* targets the host cell proteasome to suppress salicylic-acid mediated plant

defence. *PLOS Pathogens,* *9*(6), 1-22. doi: https://doi.org/10.1371/journal.ppat.1003427

Van Den Berg, N., Berger, D. K., Hein, I., Birch, P. R., Wingfield, M. J. and Viljoen, A. (2007). Tolerance in banana to Fusarium wilt is associated with early up-regulation of cell wall-strengthening genes in the roots. *Molecular Plant Pathology,* *8*(3), 333-341. doi: https://doi.org/10.1111/j.1364-3703.2007.00389.x

Van Weemen, B. K. and Schuurs, A. H. W. M. (1971). Immunoassay using antigen-enzyme conjugates. *FEBS Letters,* *15*(3), 232-236. doi: https://doi.org/10.1016/0014-5793(71)80319-8

Voigt, C. A., Schäfer, W. and Salomon, S. (2006). A comprehensive view on organ-specific callose synthesis in wheat (*Triticum aestivum* L.): glucan synthase-like gene expression, callose synthase activity, callose quantification and deposition. *Plant Physiology and Biochemistry,* *44*(4), 242-247. doi: https://doi.org/10.1016/j.plaphy.2006.05.001

Voigt, C. A. (2014). Callose-mediated resistance to pathogenic intruders in plant defense-related papillae. *Frontiers in Plant Science,* *5*(168), 1-6. doi: https://doi.org/10.3389/fpls.2014.00168

Wang, Q., Shakoor, N., Boyher, A., Veley, K. M., Berry, J. C., Mockler, T. C. and Bart, R. S. (2021). Escalation in the host-pathogen arms race: A host resistance response corresponds to a heightened bacterial virulence response. *PLOS Pathogens,* *17*(1), 1-27. doi: https://doi.org/10.1371/journal.ppat.1009175

Wang, Y., Ji, D., Chen, T., Li, B., Zhang, Z., Qin, G. and Tian, S. (2019). Production, signaling, and scavenging mechanisms of reactive oxygen species in fruit–pathogen interactions. *International Journal of Molecular Sciences,* *20*(12), 2994. doi: https://doi.org/10.3390/ijms20122994

Wi, S. J., Ji, N. R. and Park, K. Y. (2012). Synergistic biosynthesis of biphasic ethylene and reactive oxygen species in response to hemibiotrophic *Phytophthora parasitica* in tobacco plants *Plant Physiology, 159*(1), 251-265. doi: https://doi.org/10.1104/pp.112.194654

Wissemeier, A. H., Diening, A., Hergenröder, A., Horst, W. J. and Mix-Wagner, G. (1992). Callose formation as parameter for assessing genotypical plant tolerance of aluminium and manganese. *Plant and Soil, 146*(1), 67-75. doi: https://doi.org/10.1007/BF00011997

Yan, Y., Takáč, T., Li, X., Chen, H., Wang, Y., Xu, E., Xie, L., Su, Z., Šamaj, J. and Xu, C. (2015). Variable content and distribution of arabinogalactan proteins in banana (*Musa spp*.) under low temperature stress. *Frontiers in Plant Science, 6*(353). doi: https://doi.org/10.3389/fpls.2015.00353

Yun, M. H., Torres, P. S., Oirdi, M. E., Rigano, L. A., Gonzalez-Lamothe, R., Marano, M. a. R., Castagnaro, A. P., Dankert, M. A., Bouarab, K. and Vojnov, A. A. (2006). Xanthan induces plant susceptibility by suppressing callose deposition. *Plant Physiology, 141*(1), 178-187. doi: https://doi.org/10.1104/pp.105.074542

Zhang, H., Shi, W. L., You, J. F., Di Bian, M., Qin, X. M., Yu, H., Liu, Q., Ryan, P. R. and Yang, Z. M. (2015). Transgenic *Arabidopsis thaliana* plants expressing a β-1,3-glucanase from sweet sorghum (*Sorghum bicolor L*.) show reduced callose deposition and increased tolerance to aluminium toxicity. *Plant, Cell and Environment, 38*, 1178–1188. doi: https://doi.org/10.1111/pce.12472

Zhou, B., Wang, J., Guo, Z., Tan, H. and Zhu, X. (2006). A simple colorimetric method for determination of hydrogen peroxide in plant tissues. *Plant Growth Regulation, 49*(2), 113-118. doi: https://doi.org/10.1007/s10725-006-9000-2

Zvyagintseva, T. N., Shevchenko, N. M., Popivnich, I. B., Isakov, V. V., Scobun, A. S., Sundukova, E. V. and Elyakova, L. A. (1999). A new procedure for the separation of water-soluble polysaccharides from brown seaweeds. *Carbohydrate Research, 322*(1), 32-39. doi: https://doi.org/10.1016/S0008-6215(99)00206-2

Table 1. Presence (+) or absence (-) of *Xcm* in the leaves of the *Xcm*-inoculated and control plants as detected by LFDs and PCR

Time (dpi)	Kayinja	Mbwazirume	*M. balbisiana*	Controls
0	-	-	-	-
1	-	-	-	-
2	-	-	-	-
7	+	+	-	-
14	+	+	+	-
28	+	+	+	-
35	na	na	+	-
42	na	na	+	-
49	na	na	+	-
56	na	na	-	-

[na]The experimental plants had completely wilted and testing of the plants by LFD and PCR was not performed

Table 2. Quantification of callose production in the three banana genotypes inoculated with *Xcm*

Factors	Callose quantification by fluorescence microscopy (particles per mm²)						Callose quantification by ELISA (µg/mL)					
	Df_1, Df_2	*F*	*P*	Factor levels	N	X±SEM	Df_1, Df_2	*F*	*P*	Factor levels	N	X±SEM
Genotype	2,285	3.049	0.049	Kayinja	96	29.74±1.46^{a}	2,1175	1.30	0.273	Kayinja	403	2.64±0.07
				Mbwazirume	96	31.88±1.59^{ab}				Mbwazirume	383	2.81±0.08
				M. balbisiana	96	35.42±1.85^{b}				*M. balbisiana*	392	2.77±0.08
Treatment	1,286	9.43	0.0023	Control	144	29.46±1.22	1,1062	25.75	ᵀ<0.001	Control	643	2.53±0.06
				Xcm	144	35.24±1.44				*Xcm*	535	2.99±0.07
Organ	1,242.56	853.07	ᵀ<0.001	Pseudostems	144	18.34±0.51	3,542.52	1636.80	ᵀ<0.001	Pseudostems	300	2.42±0.04^{b}
				Corms	144	46.35±0.81				Corms	262	5.06±0.07^{d}
				Leaves	N/A	N/A				Leaves	330	1.16±0.01^{a}
				Roots	N/A	N/A				Roots	286	2.76±0.03^{c}
Time (dpi)	5,131.23	8.83	ᵀ<0.001	0	48	24.92±1.80^{a}	5,506.58	55.62	ᵀ<0.001	0	111	1.78±0.08^{a}
				1	48	26.15±1.85^{a}				1	243	2.03±0.07^{ab}
				2	48	29.10±2.24^{ab}				2	235	2.40±0.08^{b}
				7	48	35.41±2.22^{bc}				7	204	2.95±0.10^{c}
				14	48	39.27±2.54^{c}				14	197	3.42±0.13^{d}
				28	48	39.23±2.43^{c}				28	188	3.70±0.14^{d}

Means at each factor level followed by different letters indicate significant differences (ANOVA, ᵀWelch's ANOVA, $P \leq 0.05$). For data that violated Levene's test for homogeneity of variance, ᵀWelch's ANOVA was used. Data are shown as mean ± standard error of the mean. Experiments were performed in triplicate and repeated two times with similar results.

Table 3. Main and interaction effect sizes of the different independent factors on callose production in the three banana genotypes inoculated with *Xcm*.

Factors	Callose detection by fluorescence microscopy				Callose detection by ELISA method			
	Df_1	*F*	*P*	Partial Eta Squared (η^2_p)	Df_1	*F*	*P*	Partial Eta Squared (η^2_p)
Genotype (G)	2	336.02	<0.001	0.021	2	300.85	<0.001	0.002
Organ (O)	1	24027.78	<0.001	0.749	3	89779.5	<0.001	0.793
Time (Ti)	5	853.44	<0.001	0.133	5	9363.88	<0.001	0.138
Treatment (Tr)	1	1024.11	<0.001	0.032	1	2228.38	<0.001	0.007
G × O	2	70.21	<0.001	0.004	6	107.17	<0.001	0.002
G × Ti	10	17.31	<0.001	0.005	10	39.33	<0.001	0.001
O × Ti	5	52.69	<0.001	0.008	15	1016.87	<0.001	0.045
G × Tr	2	188.36	<0.001	0.012	2	11.33	<0.001	0
O × Ti	1	9.63	0.022	0	3	213.12	<0.001	0.002
Ti × Tr	5	113.18	<0.001	0.018	4	26.71	<0.001	0
G × O × Ti	10	9.84	<0.001	0.003	30	20.82	<0.001	0.002
G × O × Tr	2	30.54	<0.001	0.002	6	27.42	<0.001	0
G × Ti × Tr	10	12.31	<0.001	0.004	8	32.2	<0.001	0.001
O × Ti × Tr	5	2.86	0.016	0	12	50.21	<0.001	0.002
G × O × Ti × Tr	10	5.01	<0.001	0.002	24	29.16	<0.001	0.002
Residuals (Df_2)	216			0.007	1046			0.003
Total								

Table 4. H_2O_2 quantification by spectrophotometry in mol/L in the two banana genotypes inoculated with *Xcm*

Factors	Df_1,Df_2	*F*	*P*	Factor levels	N	X̄±SEM
Genotype	1,178	0.08	0.779	Kayinja	90	7.81±0.41
				Mbwazirume	90	7.65±0.39
Treatment	1,125.13	7.48	₸0.007	Control	90	6.98±0.23
				Xcm	90	8.48±0.50
Organ	2,104.59	3.88	₸0.024	Leaves	60	7.29±0.25^a
				Pseudostems	60	8.57±0.39^b
				Corms	60	7.33±0.69^a
Time (hpi)	4,86.158	25.94	₸<0.001	0	36	5.02±0.46^a
				1	36	11.79±0.68^c
				3	36	7.89±0.39^b
				6	36	5.48±0.31^a
				12	36	8.46±0.50^b

Means at each factor level followed by different letters indicate significant differences (ANOVA, ₸Welch's ANOVA, $P \leq 0.05$). For data that violated Levene's test for homogeneity of variance, ₸Welch's ANOVA was used. Data are shown as mean ± standard error of the mean. Experiments were performed in triplicate and repeated two times with similar results.

Fig. 1. BXW disease development in the three banana genotypes. Symptomless plants of non-inoculated Kayinja (**A)**, Mbwazirume (**B)** and *M. balbisiana* (**C)** and development of BXW disease symptoms (white arrowheads) in Kayinja (**D, G, J**) Mbwazirume (**E, H, K**) and *M. balbisiana* (**F, I, L**) at 14, 28 and 56 days post-inoculation (dpi) with *Xcm*. Localized hypersensitive response was observed in the inoculated leaf of *M. balbisiana* plants by 14 dpi (**F**) and remained symptomless and healthy by 56 dpi (**L**) compared to Kayinja (**top row**) and Mbwazirume (**middle row**) that displayed systemic wilting or yellowing at 14 dpi and completely dried by 56-dpi. Experiments were performed in triplicate and repeated two times with similar results. The mean number of dpi to first appearance of BXW symptoms and death of entire plants in response to *Xcm* inoculation in the three banana genotypes (ANOVA; $F_{(4,86)}$=2537, n = 21, $P < 0.001$) (**Fig. 1M**). Different letters indicate significant differences (ANOVA, ᵀWelch's ANOVA, $P \leq 0.05$).

Fig. 2. Callose production in pseudostems (**A** and **B**), corms (**C** and **D**), leaves (**E**) and roots (**F**) of *Xcm*-inoculated and control banana genotypes at 0, 2, 7, 14, and 28 days post inoculation (dpi) as assessed by fluorescence microscopy (**A** and **C**) and ELISA (**B**, **D, E** and **F**). Significant variability ($P < 0.001$) in callose production in *Xcm*-inoculated plants were observed between the genotypes (fluorescence microscopy), treatments, organs and time (dpi) (Welch's ANOVA, $P < 0.05$) while no significant difference was observed between the genotypes as assessed by the ELISA method ($P > 0.05$; Table 2). Experiments were performed in triplicate and repeated two times generating consistent results.

Fig. 3. Callose deposition in different banana genotypes in response to *Xc*m infection. Callose deposition (white fluorescing particles shown by the white arrow heads) at 14 dpi obtained by fluorescence microscopy of aniline blue stained sections of pseudostems (**A-F**), corms (**G-L**)

and roots (**M-R**) in the three banana genotypes. Callose was consistently detected in pseudostems (**A-F**) and corms (**G-L**) but not in roots (**M-R**). Callose deposition was greater in *Xcm*-inoculated plants than in control plants. All images taken at 100x magnification using an AxioScope microscope (Carl-Zeiss, Oberkochen, Germany). Scale bar represents 200 µm. Experiments were performed in triplicate and repeated two times with similar results (ANOVA, $n = 16$, $P < 0.05$).

Fig. 4. H_2O_2 production observed by 3,3'-Diaminobenzidine (DAB) staining in different tissues in response to *Xcm* infection and visualization by microscopy of H_2O_2-DAB yellow-orange precipitate in banana tissues (leaf, pseudostem, and corm) of Kayinja and Mbwazirume genotypes following inoculation with Xcm. Non-inoculated control samples (top row) and 1, 6, and 12 hpi, row 2 to 4) are shown. The brown precipitate from DAB staining accumulated in patches near vascular tissues of leaves (D-E and G-H) and pseudostems (**P**-**Q** and **V**-**W**) compared to randomly distributed vesicle-like structures across the corm tissue (**C**, **F**, **I** and **O**, **R**, **U**). All images are of magnification 50x and were taken using a Zeiss-Axiocam digital camera, mounted on AxioScope microscope (Carl-Zeiss, Oberkochen, Germany). Experiments were performed in triplicate and repeated two times generating consistent results.

Fig. 5. Quantitative variation in mean concentration of H_2O_2 (µmol/L) in the leaf (**A**), pseudostem (**B**) and corm (**C**) tissues of *Xcm*-inoculated and control plants of Kayinja and Mbwazirume as assessed between 0 and 12 hpi. All tissues showed an initial transient spike in H_2O_2 at 1 hpi followed by a decline at 3-6 hpi and second spike at 12 hpi. Differences between treatments, organs and time points were significant ($P < 0.01$) whereas they were not

significant between genotypes ($P > 0.05$) (Table 4). Experiments were performed in triplicate and repeated two times and generated consistent results.

Supplementary Fig. S1. Laminarin (**A**) and H_2O_2 (**B**) standard curves used for quantification of callose and H_2O_2 production in banana tissues, respectively. Like callose, laminarin is a 1-3-β-glucan polymer and may be used as standard callose equivalents in ELISA. The dotted line represents 95% confidence interval for the regression line.

Supplementary Fig. S2. Quantitative variation in callose and H_2O_2 production in the three banana genotypes following inoculation with *Xcm*. The mean number of callose particles per mm^2 by the fluorescence microscopy method (**A**), mean callose concentration in µg/mL by the TAS-ELISA method (**B**) and mean H_2O_2 concentration in mol/L by spectrophotometry method (**C**). All factor levels showed statistically significant variation in callose and H_2O_2 production (ANOVA and Welch's ANOVA, $P < 0.05$) except for callose production in the three banana genotype through the ELISA detection method and H_2O_2 production in the two banana genotypes ($P > 0.05$).

Supplementary Fig. S3. Callose depositions (white fluorescing particles, red arrow heads) at 14-dpi in aniline blue-stained sections with a blue background of pseudostems (**A-F**) and corms (**G-L**) of three banana genotypes as detected by fluorescence microscopy. Callose was consistently detected in pseudostems and corms fluorescing particles (**A-L**). Both *Xcm*-inoculated and control plants showed callose deposition and there was more callose in inoculated than control plants. In contrast, the fluorescing particles were not observed in the roots (**M-R**), both in *Xcm* and control plants, although callose was detected in the roots using

1320 enzyme-linked immunosorbent assay (Table 3 and 4). All images taken at 100x

1321 magnification. Scale bar represents 200 µm.

1322

1323

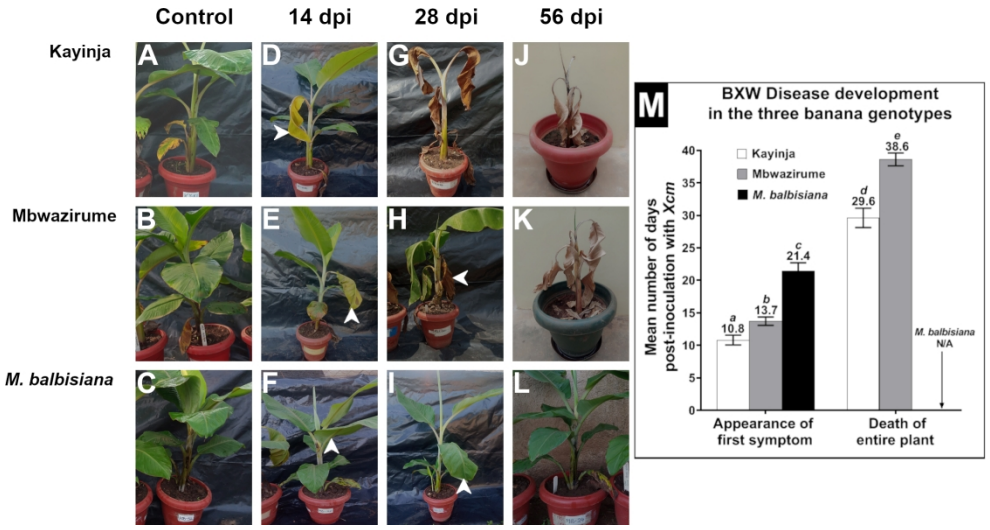

Fig. 1. BXW disease development in the three banana genotypes. Symptomless plants of non-inoculated Kayinja (A), Mbwazirume (B) and M. balbisiana (C) and development of BXW disease symptoms (white arrowheads) in Kayinja (D, G, J) Mbwazirume (E, H, K) and M. balbisiana (F, I, L) at 14, 28 and 56 days post-inoculation (dpi) with Xcm. Localized hypersensitive response was observed in the inoculated leaf of M. balbisiana plants by 14 dpi (F) and remained symptomless and healthy by 56 dpi (L) compared to Kayinja (top row) and Mbwazirume (middle row) that displayed systemic wilting or yellowing at 14 dpi and completely dried by 56-dpi. Experiments were performed in triplicate and repeated two times with similar results. The mean number of dpi to first appearance of BXW symptoms and death of entire plants in response to Xcm inoculation in the three banana genotypes (ANOVA; $F(4,86)=2537$, $n = 21$, $P < 0.001$) (Fig. 1M). Different letters indicate significant differences (ANOVA, ₸Welch's ANOVA, $P \leq 0.05$).

193x99mm (300 x 300 DPI)

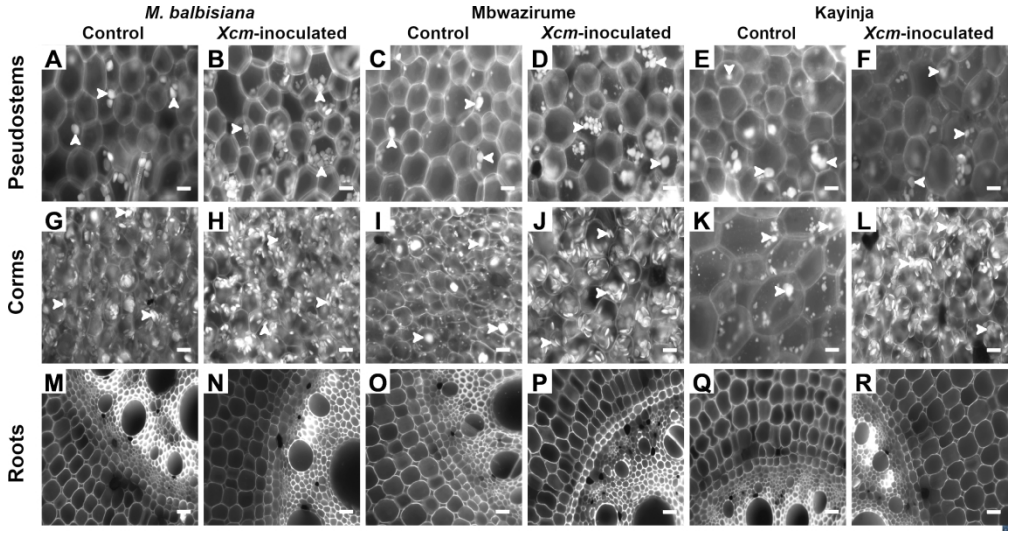

Fig. 2. Callose production in pseudostems (A and B), corms (C and D), leaves (E) and roots (F) of Xcm-inoculated and control banana genotypes at 0, 2, 7, 14, and 28 days post inoculation (dpi) as assessed by fluorescence microscopy (A and C) and ELISA (B, D, E and F). Significant variability ($P < 0.001$) in callose production in Xcm-inoculated plants were observed between the genotypes (fluorescence microscopy), treatments, organs and time (dpi) (Welch's ANOVA, $P < 0.05$) while no significant difference was observed between the genotypes as assessed by the ELISA method ($P > 0.05$; Table 2). Experiments were performed in triplicate and repeated two times generating consistent results.

243x127mm (300 x 300 DPI)

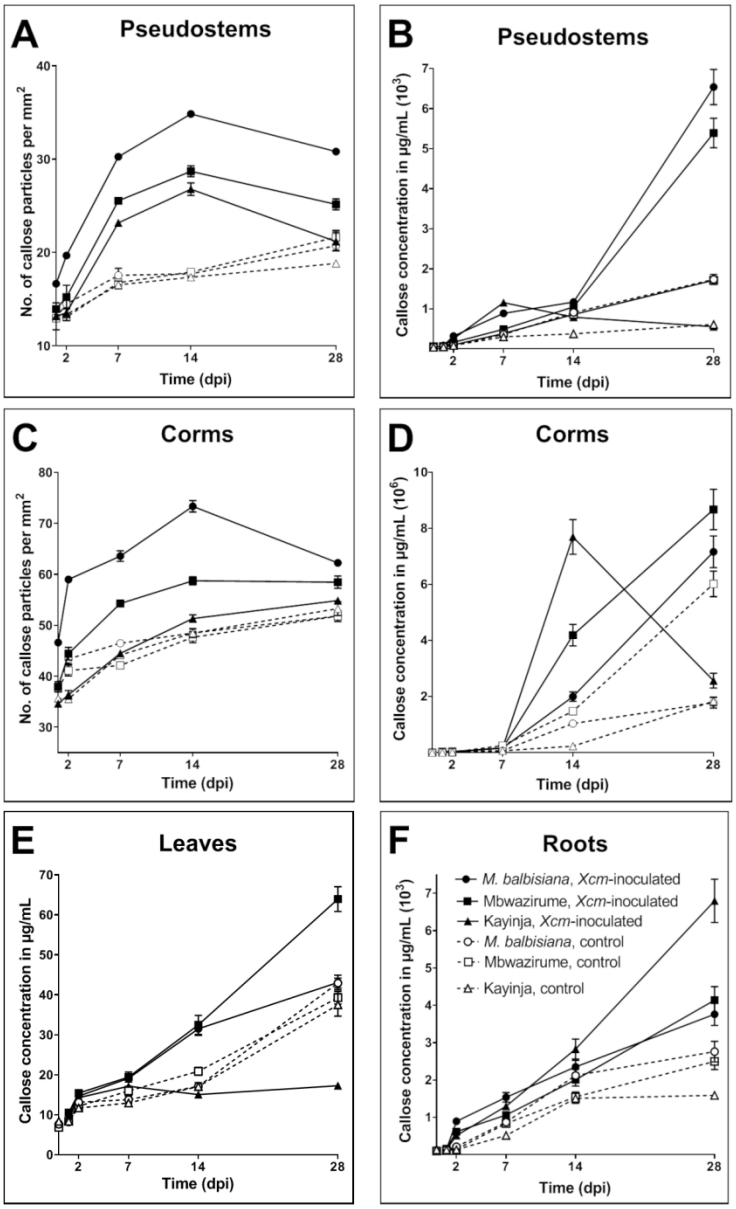

Fig. 3. Callose deposition in different banana genotypes in response to Xcm infection. Callose deposition (white fluorescing particles shown by the white arrow heads) at 14 dpi obtained by fluorescence microscopy of aniline blue stained sections of pseudostems (A-F), corms (G-L) and roots (M-R) in the three banana genotypes. Callose was consistently detected in pseudostems (A-F) and corms (G-L) but not in roots (M-R). Callose deposition was greater in Xcm-inoculated plants than in control plants. All images taken at 100x magnification using an AxioScope microscope (Carl-Zeiss, Oberkochen, Germany). Scale bar represents 200 µm. Experiments were performed in triplicate and repeated two times with similar results (ANOVA, n = 16, $P < 0.05$).

102x167mm (300 x 300 DPI)

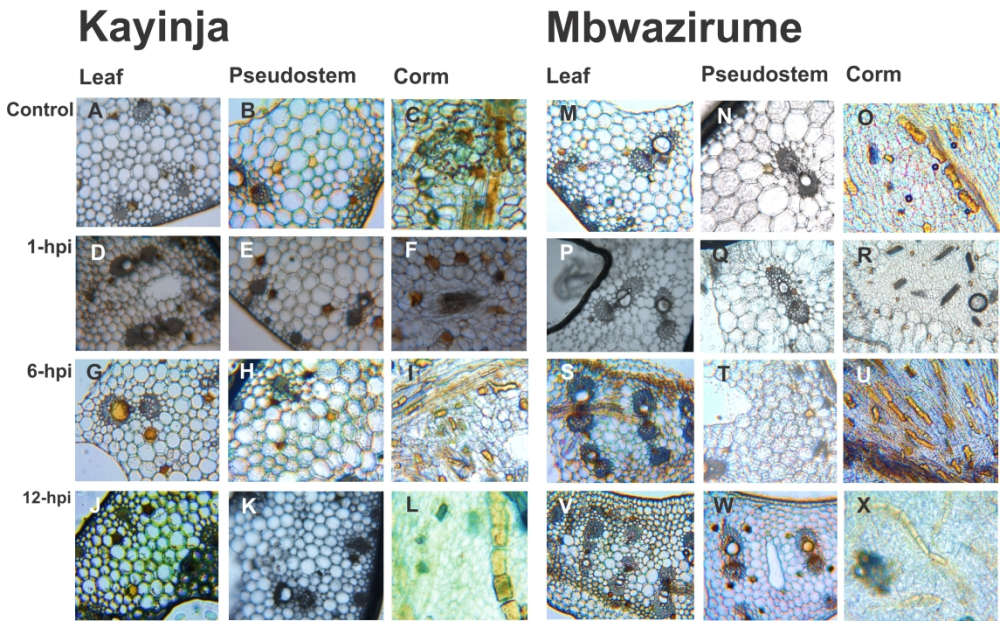

Fig. 4. H2O2 production observed by 3,3'-Diaminobenzidine (DAB) staining in different tissues in response to Xcm infection and visualization by microscopy of H2O2-DAB yellow-orange precipitate in banana tissues (leaf, pseudostem, and corm) of Kayinja and Mbwazirume genotypes following inoculation with Xcm. Non-inoculated control samples (top row) and 1, 6, and 12 hpi, row 2 to 4) are shown. The brown precipitate from DAB staining accumulated in patches near vascular tissues of leaves (D-E and G-H) and pseudostems (P-Q and V-W) compared to randomly distributed vesicle-like structures across the corm tissue (C, F, I and O, R, U). All images are of magnification 50x and were taken using a Zeiss-Axiocam digital camera, mounted on AxioScope microscope (Carl-Zeiss, Oberkochen, Germany). Experiments were performed in triplicate and repeated two times generating consistent results.

296x183mm (300 x 300 DPI)

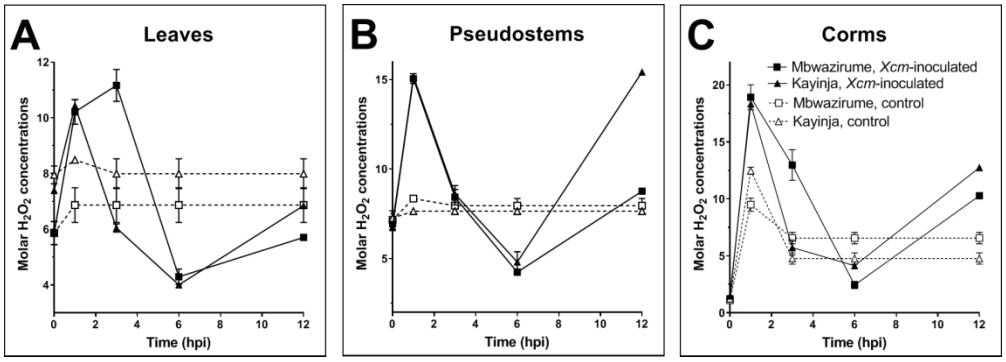

Fig. 5. Quantitative variation in mean concentration of H2O2 (µmol/L) in the leaf (A), pseudostem (B) and corm (C) tissues of Xcm-inoculated and control plants of Kayinja and Mbwazirume as assessed between 0 and 12 hpi. All tissues showed an initial transient spike in H2O2 at 1 hpi followed by a decline at 3-6 hpi and second spike at 12 hpi. Differences between treatments, organs and time points were significant ($P < 0.01$) whereas they were not significant between genotypes ($P > 0.05$) (Table 4). Experiments were performed in triplicate and repeated two times and generated consistent results.

156x54mm (300 x 300 DPI)

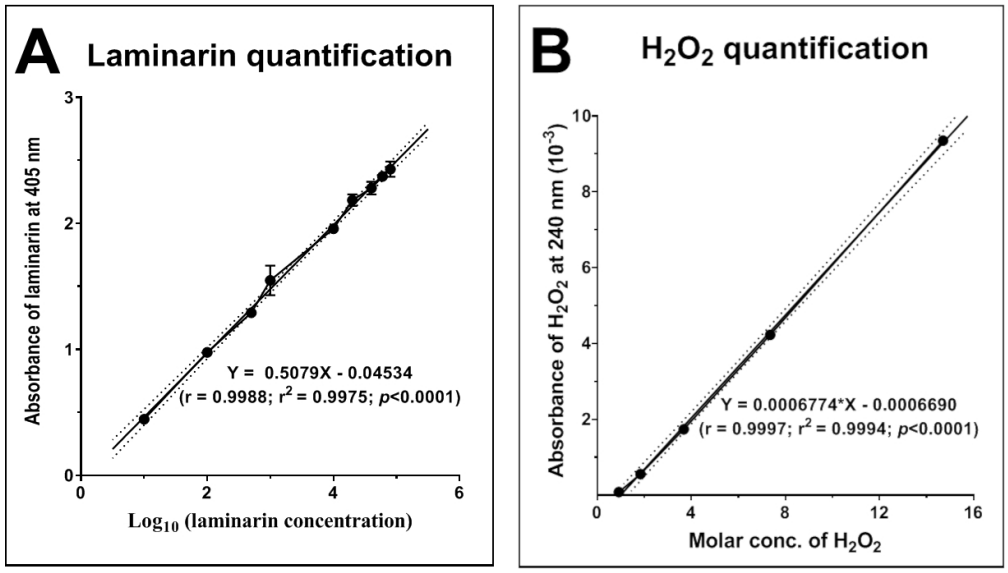

Supplementary Fig. S1. Laminarin (A) and H2O2 (B) standard curves used for quantification of callose and H2O2 production in banana tissues, respectively. Like callose, laminarin is a 1-3-β-glucan polymer and may be used as standard callose equivalents in ELISA. The dotted line represents 95% confidence interval for the regression line.

103x58mm (300 x 300 DPI)

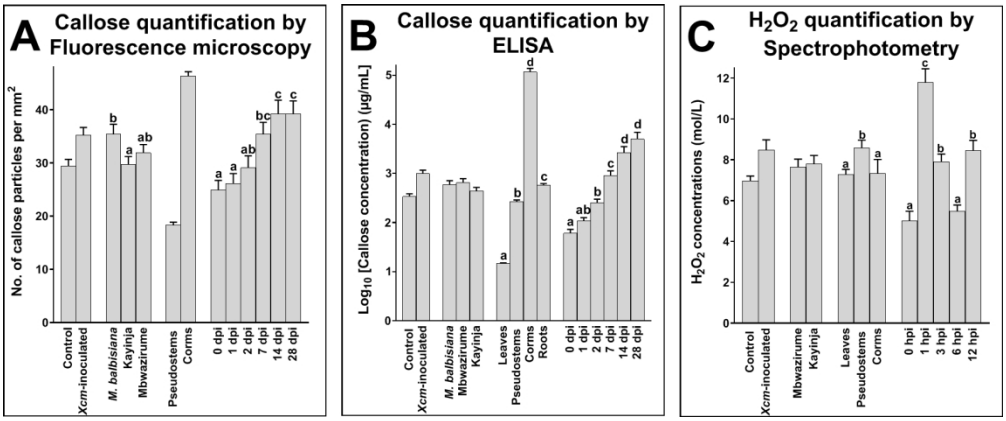

Supplementary Fig. S2. Quantitative variation in callose and H2O2 production in the three banana genotypes following inoculation with Xcm. The mean number of callose particles per mm2 by the fluorescence microscopy method (A), mean callose concentration in µg/mL by the TAS-ELISA method (B) and mean H2O2 concentration in mol/L by spectrophotometry method (C). All factor levels showed statistically significant variation in callose and H2O2 production (ANOVA and Welch's ANOVA, $P < 0.05$) except for callose production in the three banana genotype through the ELISA detection method and H2O2 production in the two banana genotypes ($P > 0.05$).

159x65mm (300 x 300 DPI)

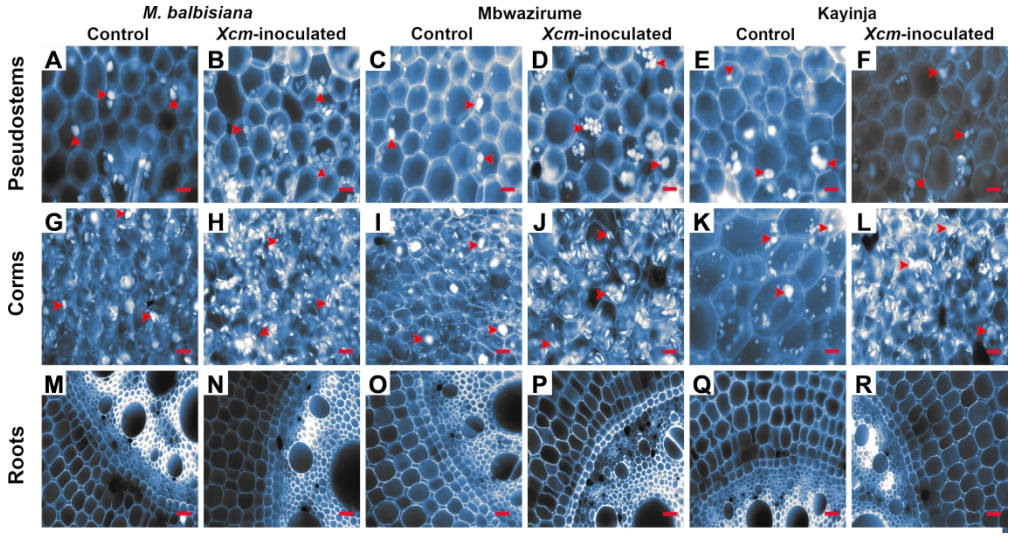

Supplementary Fig. S3. Callose depositions (white fluorescing particles, red arrow heads) at 14-dpi in aniline blue-stained sections with a blue background of pseudostems (A-F) and corms (G-L) of three banana genotypes as detected by fluorescence microscopy. Callose was consistently detected in pseudostems and corms fluorescing particles (A-L). Both Xcm-inoculated and control plants showed callose deposition and there was more callose in inoculated than control plants. In contrast, the fluorescing particles were not observed in the roots (M-R), both in Xcm and control plants, although callose was detected in the roots using enzyme-linked immunosorbent assay (Table 3 and 4). All images taken at 100x magnification. Scale bar represents 200 µm.

243x128mm (300 x 300 DPI)